ERDC/CHL TR-22-14

US Army Corps
of Engineers®
Engineer Research and
Development Center

Regional Sediment Management Program

Using Geophysical and Erosion Properties to Identify Potential Beneficial Use Applications for Atlantic Intracoastal Waterway Sediments

David W. Perkey, Danielle R. N. Tarpley, and Renée M. Styles

July 2022

Coastal and Hydraulics Laboratory

The US Army Engineer Research and Development Center (ERDC) solves the nation's toughest engineering and environmental challenges. ERDC develops innovative solutions in civil and military engineering, geospatial sciences, water resources, and environmental sciences for the Army, the Department of Defense, civilian agencies, and our nation's public good. Find out more at www.erdc.usace.army.mil.

To search for other technical reports published by ERDC, visit the ERDC online library at https://erdclibrary.on.worldcat.org/discovery.

ERDC/CHL TR-22-14
July 2022

Using Geophysical and Erosion Properties to Identify Potential Beneficial Use Applications for Atlantic Intracoastal Waterway Sediments

David W. Perkey, Danielle R. N. Tarpley, and Renée M. Styles

Coastal and Hydraulics Laboratory
US Army Engineer Research and Development Center
3909 Halls Ferry Road
Vicksburg, MS 39180-6199

Final report

Prepared for Regional Sediment Management Program
US Army Engineer Research and Development Center
Vicksburg, MS 39180-6199

Under Funding Account code U4375439; AMSCO Code 008303

Abstract

In an effort to identify alternative and beneficial use placement strategies for dredged sediments from the Atlantic Intracoastal Waterway (AIWW), the US Army Corps of Engineers, Savannah District (SAS), and the US Army Engineer Research and Development Center (ERDC) performed a series of physical property tests of 34 core borings from the SAS AIWW. Physical property testing found that 14 of the borings were non-cohesive sandy materials that may be suitable for potential beach renourishment or berm construction. The remaining 20 borings had mud contents sufficient enough to result in cohesive behavior. A subset of six of these materials from across the geographic region were further evaluated to characterize their erosion behavior.

Following a self-weight consolidation period of 30 days, erosion testing showed that the tested cohesive sediments had critical shear stress values that ranged from 1.7 Pa to 2.9 Pa, suggesting that these sediments would likely be resistant to erosion in most wetland environments after placement. Additionally, the cohesive sediments were found to produce gravel-sized mud clasts. These clasts could account for 20% or more of the eroded mass and significantly reduce the amount of silts and clays incorporated in suspended plumes during and immediately following placement.

Contents

Figures and Tables

Figures

Tables

Preface

This study was conducted for the Regional Sediment Management (RSM) Program "Identification of Dredged Material Beneficial Uses from Geophysical Analysis of Sediment Borings" under Funding Account Code U4375439; AMSCO Code 008303.

The work was performed by the Field Data Collection and Analysis Branch of the Navigation Division, US Army Engineer Research and Development Center, Coastal and Hydraulics Laboratory (ERDC-CHL). At the time of publication of this report, Mr. William Butler was chief of the Field Data Collection and Analysis Branch; Ms. Ashley Frey was chief of the Navigation Division; and Mr. Charles E. Wiggins was the technical director for Navigation. The deputy director of ERDC-CHL was Mr. Keith Flowers, and the director was Dr. Ty V. Wamsley.

The commander of ERDC was COL Christian Patterson, and the director was Dr. David W. Pittman.

1 Introduction

1.1 Background

Effective sediment management within the nation's navigable waterways and coastal areas is an important mission to the US Army Corps of Engineers (USACE). Recent changes in policy (e.g., The Water Resources Development Act of 2020) are encouraging the USACE to find more ways to beneficially use the sediments it dredges and reduce placement within inland and offshore disposal locations. In response to this policy, the USACE Savannah District (SAS) and the US Army Engineer Research and Development Center (ERDC) are currently investigating potential Beneficial Use of Dredged Material (BUDM) applications for sediments being dredged from the Atlantic Intracoastal Waterway (AIWW).

The AIWW is a vital marine highway along the Atlantic coast, providing safe navigation for commercial and recreational vessels. Approximately 22% of the AIWW is managed by the SAS. Historically, the primary method of the disposal of dredged material for the district was undiked discharge into tracts adjacent to the waterway. However, this disposal method is unsustainable since >35% of operational reaches within the SAS portion of the AIWW lack 20 yr[1] disposal area capacity. Projects that use dredge materials in building bird islands, marsh restoration/development, restoring eroded shorelines, or thin layer, deep hole or near shore placement are all potential options that could be both beneficial and sustainable.

In May of 2021, SAS contracted GHD Inc. to collect 34 vibracores from a stretch of the AIWW between Beaufort County, South Carolina, and Camden County, Georgia (Figure 1). A complete description of the core collection effort can be found in Appendix C. These cores provided test sediments for geophysical and erosional characterization of bottom sediments to guide decisions on the materials and reaches of the AIWW that are most appropriate for various types of BUDM projects for the area. The presence and formation of mud aggregates during dredging and

[1] For a full list of the spelled-out forms of the units of measure used in this document, please refer to *US Government Publishing Office Style Manual*, 31st ed. (Washington, DC: US Government Publishing Office 2016), 248-52, https://www.govinfo.gov/content/pkg/GPO-STYLEMANUAL-2016/pdf/GPO-STYLEMANUAL-2016.pdf.

placement is of particular interest to SAS as these clasts have been shown to have limited mobility that would largely be limited to bedload transport within the area (Perkey et al. 2020a). These properties are viewed as positive features in the building of bird islands.

Figure 1. Regional map of test sediment locations. Blue triangles mark sample locations that were used in this study for erosion analysis. Red dots indicate the locations of the other vibracores.

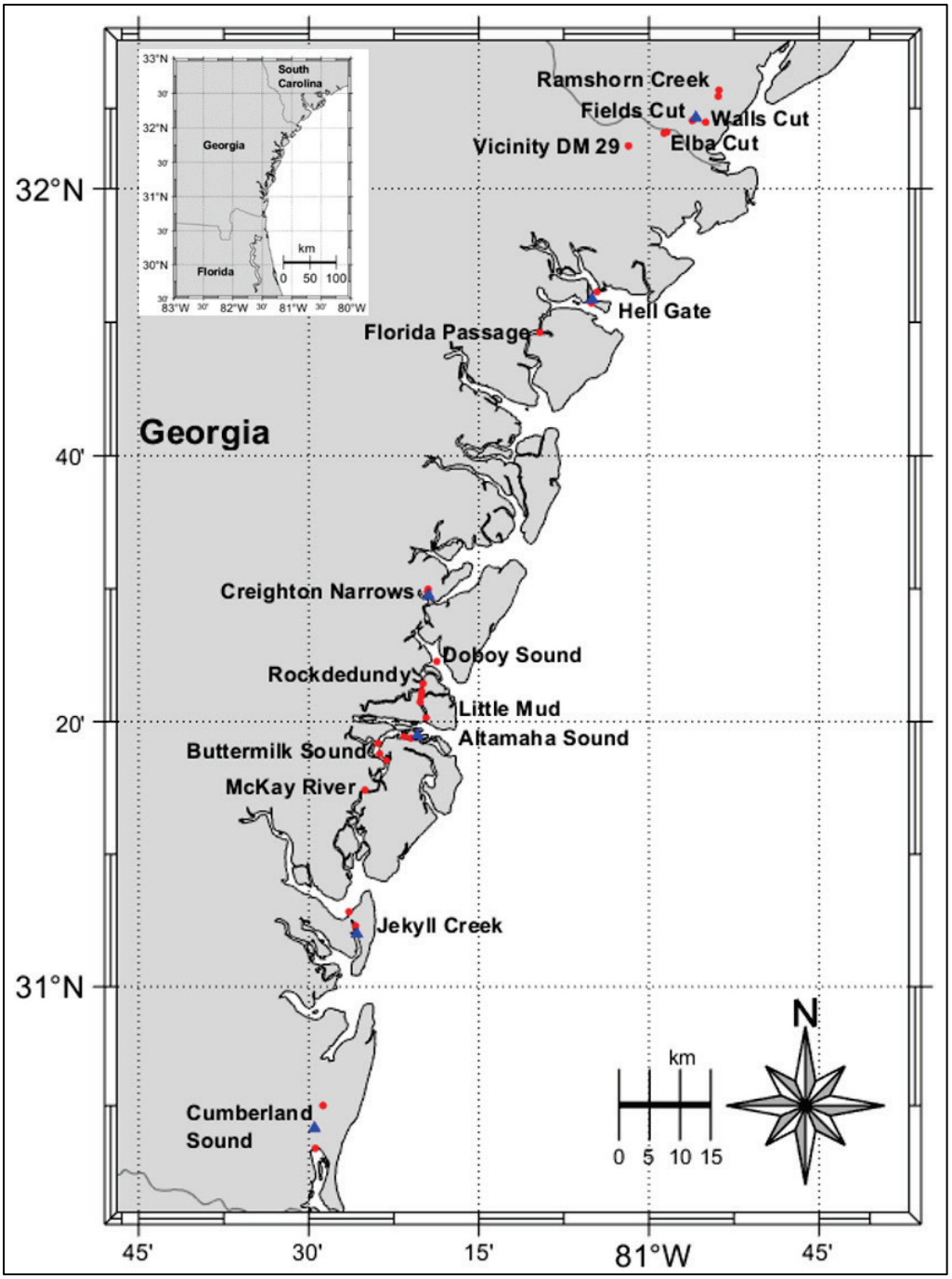

1.2 Objective

The goal of this study is to expand the data set of the geophysical and erosional properties of bottom sediments from within the AIWW and use this information to identify the most appropriate BUDM projects for these materials.

1.3 Approach

Standard laboratory methods were used to evaluate the geophysical properties of the sediments obtained from 34 AIWW borings. Analyses included grain size, moisture content, organic content via Loss-On-Ignition (LOI), and Atterberg limits. Following initial evaluation of these properties, a subset of six samples was selected for further flume-based erosion and mud aggregate production testing with the USACE-developed Sedflume (McNeil et al. 1996) coupled with the Flume Imaging Camera System (FICS) (Perkey et al. 2020a,c; Fall et al. 2020). Additionally, the durability of aggregates composed of these sediments was evaluated with a modified Slake Durability tumbling device.

2 Methods

The 34 vibracore borings for this study were collected by GHD Inc. from May 19–24, 2021. Recovered sediments from each location were extruded into 5 gal[1] buckets and shipped to ERDC Coastal and Hydraulics Laboratory (CHL) in Vicksburg, Mississippi. The sediment samples were received May 27, 2021, and visually inspected to confirm no damage or loss occurred during shipping. The contents of each bucket were homogenized in the ERDC-CHL sediment laboratory and subsampled for testing described in the following sections.

2.1 Physical properties

2.1.1 Water content and bulk density

Water content (w) of each sample was measured through wet-dry weight analysis following ASTM D2216-19 (2019) in which w is given by

$$w = \left(\frac{m_w - m_d}{m_d} \right) \tag{1}$$

where m_w and m_d are the wet and dry weights, respectively. The total volume of sample was assumed to consist of both solid particles and water, with assumed densities of 2.65 g/cm^3 and 1.0 g/cm^3, respectively. The bulk density as a function of w and the densities of the solid particles (ρ_s) and water (ρ_w) was calculated with Equation 2, derived from Jepsen et al. (2010).

$$\rho = \rho_s + \frac{w\rho_s \left(\rho_w - \rho_s \right)}{\rho_w + w\rho_s} \tag{2}$$

2.1.2 Plasticity Index (PI)

The Plasticity Index (PI) of each material was obtained through standard Atterberg Limit testing. Standard methods, described in ASTM D4318-05 (2015), were utilized to measure the liquid and plastic limits. To obtain the

[1] For a full list of the unit conversions used in this document, please refer to *US Government Publishing Office Style Manual*, 31st ed. (Washington, DC: US Government Publishing Office 2016), 345-7, https://www.govinfo.gov/content/pkg/GPO-STYLEMANUAL-2016/pdf/GPO-STYLEMANUAL-2016.pdf.

liquid limit, the multipoint method was utilized with a motorized device to maintain a constant drop rate. Plastic limit testing was conducted on a polished granite countertop using the hand method. The difference between the two limits yields the PI for each sample, which indicates the breadth of moisture content for which the material behaves plastically.

2.1.3 Organic content

To evaluate the total, volatile organic content of the sediment samples, LOI techniques described in ASTM D2974-14 (2014), method C, were used. Following recommendations reported by Schumacher (2002) and Salehi et al. (2011), combustion temperature was reduced from 440°C down to 360°C.

2.1.4 Grain size

Grain size distributions (GSD) and characterizations were obtained through Laser Diffraction Particle Size Analysis (LDPSA), dry sieving, or a combination of the two. These data were used to determine the median grain size (D_{50}) and percentage of sand (>63 μm), silt (63-4 μm), and clay (<4 μm) sized particles (Wentworth 1929) for each sample.

Grain size distributions through LDPSA was performed using a Malvern Mastersizer 3000E, which measures particle sizes in terms of equivalent spherical diameters (esd) between the range of 0.1 to 1000 μm. Sediments were homogenized and disaggregated overnight in a solution of sodium metaphosphate (40 g/L). To remove macro-organic material, samples were passed through a 1000 μm sieve into the instrument's reservoir and sonicated for 60 sec prior to analysis.

Visual inspection of the AIWW sediments revealed that 12 of the 34 samples contained material that was too coarse for LDPSA grain size analysis and required sieving (indicated in Table 2). Standard methods described in ASTM D6913M-17 (2017) were used to dry sieve 5 of the 12 samples at 1ϕ intervals from 2000 μm to 63 μm. However, the mud (<63 μm) content in the remaining seven samples was determined to be significant and required a combination of LDPSA and sieving. For these sediments, the water content (described in Section 2.1.1) was used to calculate a total dry mass of a subsample for GSD analysis. The subsample was wet-screened through a 1000 μm sieve. Sediments passing through the sieve were analyzed with LDPSA while sediments retained on the sieve

were dried and weighed. The results of the LDPSA were adjusted using the mass fraction of the subsample analyzed via LDPSA, and the resultant mass fraction of the sieve data was appended to the adjusted LDPSA data to yield the final GSD.

2.2 Erosion testing

2.2.1 Core preparation

The general guidelines for preparing sediment mixtures for erosion testing is to sufficiently homogenize the sample to minimize down-core variability of sediment properties that would otherwise affect erosion behavior. To achieve this, all sediment samples were mixed for a minimum of 30 min before being transferred into 10 cm diameter polycarbonate tubes. Prior to placing sediment in the tube, a plunger with bentonite paste (for sealing and lubrication) was inserted into the bottom of the core.

Two methods were utilized in the transfer of sediment to the core tubes for erosion testing. For mixtures that displayed fluid behavior, the sample was poured through a funnel and pipe, which was inserted into the core tube, allowing the sediment column to be filled from the bottom up and minimize gas entrapment. For samples with higher sand and lower water contents that displayed more granular consistency, samples were tamped into the core tube in approximately 1 to 2 cm lifts. After filling the core tubes, overlying water was placed on top of the sediment column, and the prepared cores were allowed to consolidate in a 4°C cooler for approximately 30 days prior to erosion. Table 1 provides sample preparation method information for each of the cores.

Table 1. Prepared test cores.

Sample Name	Preparation Method	Date Prepared	Date Eroded
Cumberland Sound RG	Tamped Lifts	7/9/2021	8/11/2021
Northend Fields Cut	Tamped Lifts	7/9/2021	8/12/2021
Creighton Narrows DM 156	Poured Slurry	7/9/2021	8/11/2021
Hell Gate DM 89	Poured Slurry	7/9/2021	8/10/2021
Jekyll Creek DM 19	Poured Slurry	7/9/2021	8/10/2021
Altamaha Sound DM 204-206	Poured Slurry	7/9/2021	8/9/2021

2.2.2 Sedflume

All erosion testing was performed with the USACE-developed Sedflume, which is a derivative of the flume developed by researchers at the University of California at Santa Barbara (McNeil et al. 1996). The flume includes an 80 cm long inlet section (Figure 2) with cross-sectional area of 2 × 10 cm for uniform, fully developed, smooth-turbulent flow, as described in McNeil et al. (1996). The inlet section is followed by a test section with a 10 cm diameter open bottom. Coring tubes and flume test section, inlet section, and exit sections are constructed of clear polycarbonate materials to permit observation of sediment-water interactions during the course of erosion experiments. The flume includes a port over the test section to provide access to the core surface for physical sampling. The flume accepts sediment cores up to 80 cm in length.

Figure 2. Images of the Sedflume (upper left), erosion surface (lower left), and operator (lower center), along with operational test range of the flume (right).

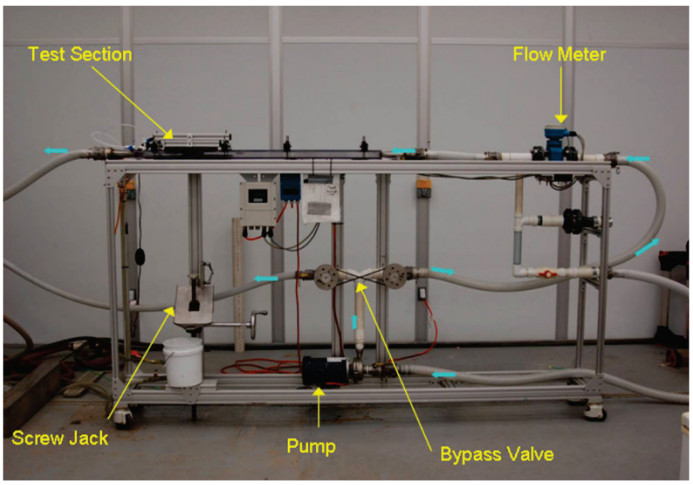

Shear Stress (Pa)	Flow Rate (GPM)
0.1	5.2
0.2	7.9
0.4	11.5
0.8	17.8
1.5	25.8
1.0	20.3
1.5	25.8
2.0	30.6
2.5	34.9
3.0	38.8
4.0	46.0
5.0	52.4
6.0	58.3
8.0	69.1
10.0	78.8
12.0	87.7

Cores are inserted into the testing section of Sedflume, and a screw jack is used to advance the plunger such that the core surface becomes flush with the bottom wall of the flume. Flow is directed over the sample by diverting water from a pump through a 5 cm inner diameter hose, into the flume. The flow through the flume produces shear stress on the surface of the core. Numerical, analytical, and experimental analyses have been performed to relate flow rate to bottom shear stress (Figure 2). As sediment is eroded from the core surface, the operator advances the screw jack to maintain the sediment surface flush with the bottom wall of the erosion flume. Erosion experiments are performed by repeating a sequence of increasing shear stresses. Approximately 1 – 5 mm of sediment is eroded at each specified shear stress; thus, the duration of each test is dependent on the rate of erosion. A diagram depicting this erosion test process along with an example erosion sequence is shown in Figure 3.

Figure 3. Diagram of sediment core erosion process. The brown arrow indicates advancement of sediment into the flume with erosion. The blue arrow indicates flow direction of water. An example erosion sequence is provided in the table to the right of the sediment core.

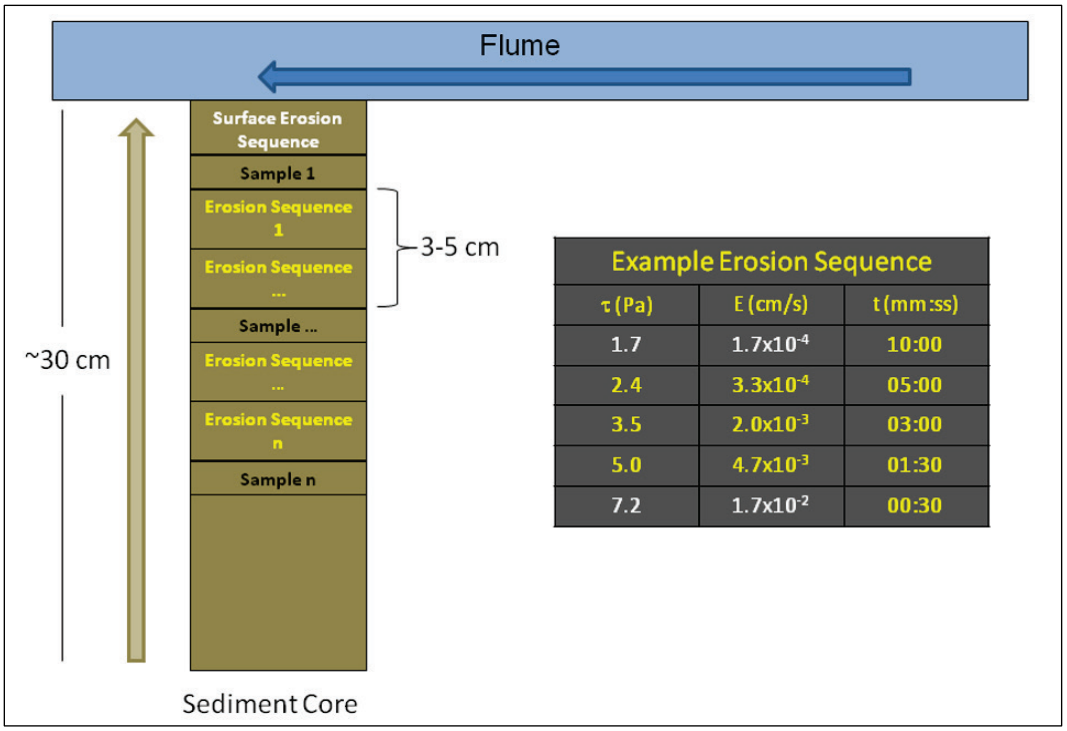

The goal of the erosion data analysis is to determine the critical shear stress (τ_{cr}) and erosion rates of cohesive sediments from the AIWW to better understand their remobilization potential following placement. Logarithmic regressions of erosion rate versus applied shear stress are performed to determine coefficients for a common cohesive sediment erosion expression. In this study, the data were fit to the Sedflume erosion power-law expression, $E=A\tau^n$ where E is erosion rate in cm/s, τ is the applied shear stress in Pa, and A and n are parameters determined from the logarithmic regression fit to the data. Critical shear stress, τ_{cr}, is determined from the regression parameters such that τ_{cr} is the shear stress that corresponds to an erosion rate, E_c of 10^{-4} cm/sec (or 3.6 mm/hr).

2.2.3 Eroded particle imaging

The FICS is an ERDC-developed system designed to characterize grain size distributions of sediment particles immediately following mobilization from the bed (Figure 4). The FICS consists of a clear polycarbonate channel, an Allied Vision, Manta G504B camera equipped with an Opto Engineering TC23056 bi-telecentric lens, and an Allied Vision LED back light paired with a Pulsar 320 strobe controller. The FICS channel is designed to attach directly to the outflow end of the Sedflume. It measures 22.5 cm in length and has the same 2 × 10 cm cross-sectional area as the Sedflume channel. The camera and lens are centrally mounted 12.8 cm above the top of the channel. FICS images an area of 4.5 × 5.3 cm, with a focal depth of 2.7 cm. Magnification of the system is 0.157×, resulting in a subject pixel size of ~22 μm. Videos were collected at a rate of three frames per second, with an exposure of 500 μs and gain set to 10. The backlight was pulsed with 24 V, 50 A with a pulse width of 30 μs. FICS videos had a default length of 240 frames (80 sec) and were collected at every erosion interval. In cases where the erosion interval duration was less than 80 sec, video collection was terminated early. For longer erosion intervals (duration exceeding 5 min), multiple videos were collected approximately every 5 min.

Figure 4. (A) Schematic showing the FICS system mounted to the outflow end of the Sedflume, and (B) the effluent collection tank.

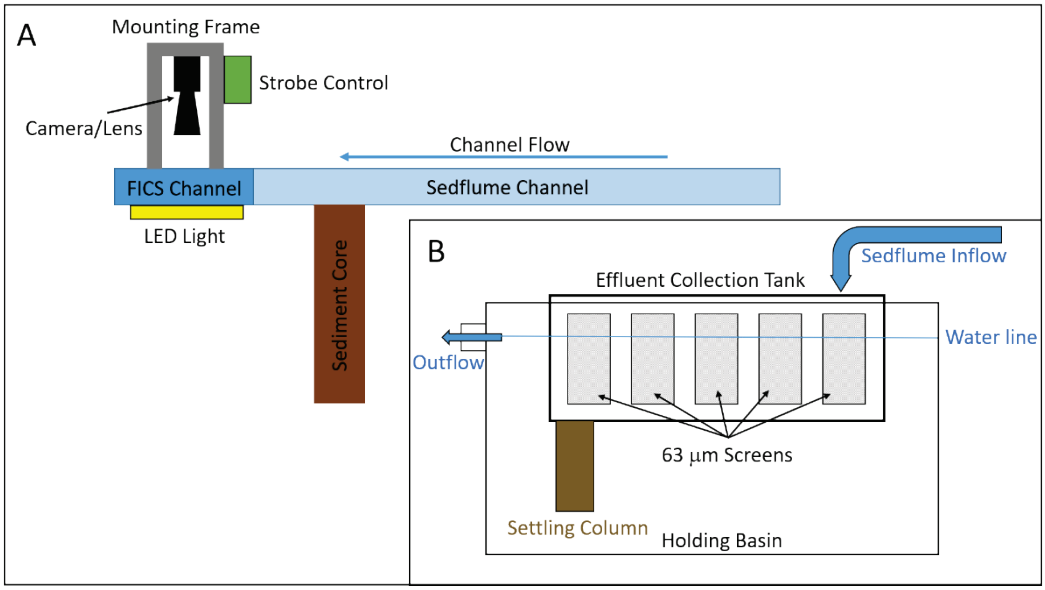

An automated image analysis routine was used to characterize the size of eroded particles in FICS images. Prior to erosion testing, a calibration grid was inserted into the FICS channel and photographed for the purpose of transforming pixel space to length. The processing routine utilizes this gridded image and employs algorithms from the MATLAB Image Processing Toolbox. It combines local intensity thresholding with particle vetting to identify particles while omitting unwanted features such as background objects, air bubbles, and out-of-focus particles. FICS image processing requires particles to appear in an area of at least 3 × 3 pixels. Therefore, the system can only accurately size particles with an esd greater than approximately 66 μm.

Prior to the start of erosion testing, background FICS videos of site water were recorded to account for any sediment particles present in the water not associated with bed erosion. To analyze the imaged particles, 48 logarithmically spaced particle size bins were generated that spanned the size range of 63 to 16000 μm. These bin properties were used to generate a volume-based particle size distribution for all the FICS videos. FICS distributions obtained from background videos were subtracted from videos recorded during erosion testing to produce a net distribution representative of eroded particles. These distributions were used to obtain the median size of eroded particles observed by the FICS (D_{50F}). Further details on these processing techniques can be found in Smith and Friedrichs (2011) and Fall et al. (2020).

2.2.4 Eroded sediment collection

Following completion of erosion data collection, additional testing was conducted with the Sedflume to evaluate the mass fraction of eroded material that occurred in an aggregate form. Flow in the flume was such that the applied shear stress on the bed produced ~2 – 3 mm of erosion over a period of 1 to 2 minutes. Effluent from the Sedflume was captured in a 129 L acrylic collection tank with 63 μm screen windows along the walls to allow water and fine suspended sediment to drain. The tank was semi-immersed in water within a larger holding basin positioned under the outflow of the flume, approximately 2 m downstream of the erosion test bed (Figure 4B).

Particles >63 μm were retained within the tank and swept to a submerged vertical settling column that held a stack of 250 μm and 63 μm sieves (Figure 4B). Sediment retained on each sieve was dried and weighed to obtain the eroded mass between 63 μm to 250 μm and >250 μm. Additionally, during the erosion event, a suspended sediment sample was obtained from within the collection tank with a peristaltic pump equipped with a 63 μm filter on the intake hose. Flow rate on the peristaltic pump was set so that a 1 to 2 L sample was collected over the entirety of the collection event. The water sample was analyzed following ASTM D3977 methods for suspended sediment concentration (SSC) analysis. The flow rate of the Sedflume and duration of the collection event was used to calculate a total volume of water passed through the collection tank. This volume was multiplied by the SSC to yield the total mass of eroded sediment <63 μm.

The resultant mass fractions of sediments <63 μm, 63 – 250 μm, and >250 μm from the erosion testing were compared to similar mass fractions obtained by wet sieving the test materials through a 63 μm and 250 μm sieve. Differences in fractions >250 μm were used to indicate the fraction of mass eroded in a macro-aggregate state.

2.3 Aggregate durability

The durability of mud aggregates was evaluated using a Slake Durability tumbler. This tumbler is a device that consists of a steel mesh drum (14 cm diameter) that is partially immersed in a water bath and rotated at a speed of 20 rpm. The apparatus is designed for the testing of shales and similar weak rock fragments. A detailed description of the device can be found in

ASTM D4644-87 (1998). For the purposes of evaluating bed aggregates in this study, the standard 2 mm wire mesh of the rotating drum was replaced with 250 μm mesh.

For each sample, cube-like aggregates of ~1 cm^3 in volume were prepared by extruding and slicing test material from the remaining sediment in the core tube following erosion testing (Figure 5a). In some instances, slicing was not possible, initially, as the water content was too high. Thus, w was reduced with a heat gun through an iterative process until the consistency of the material allowed for slicing and aggregate preparation. These samples are indicated with an asterisk (*) in Table 9. Typically, five aggregates were used for each durability test (Figure 5b). Aggregates were tumbled at intervals of 2.5, 5, 10, and 20 min (Figure 5c), which approximately correspond to linear tumbling distances of 25 m, 50 m, 100 m, and 200 m, respectively. At the completion of each tumbling interval, the drum was removed from the water bath, and the remaining contents >250 μm were filtered through pre-weighed, 90 mm diameter glass fiber filters with retention rating of 0.7 μm. Similarly, the contents of the water basin (<250 μm) were filtered through pre-weighed glass fiber filters with retention rating of 0.7 μm. Filters were dried in a 50°C oven overnight before obtaining final dry masses of fractions >250 μm and <250 μm.

Standard wet sieving techniques were used on an aliquot of each test material to assess the mass fraction >250 μm prior to aggregate durability testing (ASTM D6913M-17 2017). This fraction was subtracted from the mass fraction retained within the tumbler basket to yield a net mass fraction >250 μm ($F_{Ma\ >250}$) due to the aggregated state of the sediment.

Figure 5. Prepared mud aggregates (A) placed in test drum, (B) and tumbled in water bath, (C) for durability testing.

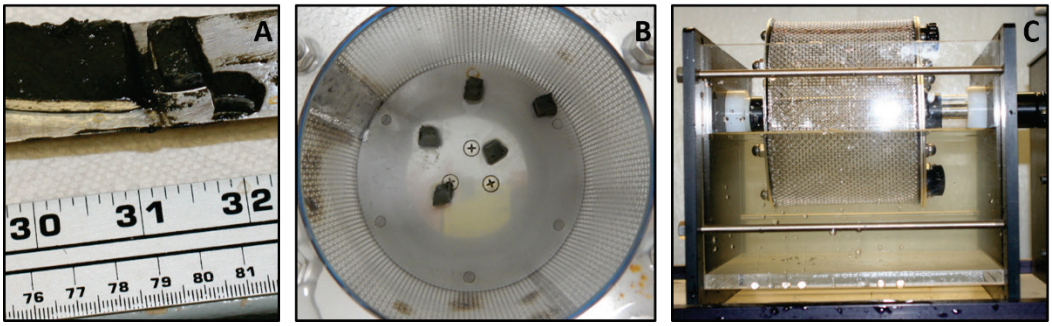

3 Results

3.1 Physical properties of test materials

The results of the physical properties measured for each vibracore material are presented in this section. A brief description of the findings obtained for each property is presented first, followed by the summarization of all physical property data in Table 2.

3.1.1 Water content and bulk density

Wet-dry analyses of the AIWW sediments showed that w ranged from 0.15 to 2.16, and corresponding bulk densities ranged from 2.18 to 1.25 g/cm^3. As shown in equation 2, ρ and w are inversely related, such that samples with the lowest w have the highest bulk density values. Water content and bulk density were also shown to be correlated with sand content (r^2=0.84 and 0.94, respectively) (Figure 6). This correlation is because fine-grained sediments have a higher porosity and capacity to hold water than sediments with a large sand fraction. Therefore, samples with more sand content had lower water content values and higher bulk densities. A complete listing of the water content and bulk density results is presented in Table 2.

Figure 6. Correlation between water content (A) and bulk density (B) with sand content.

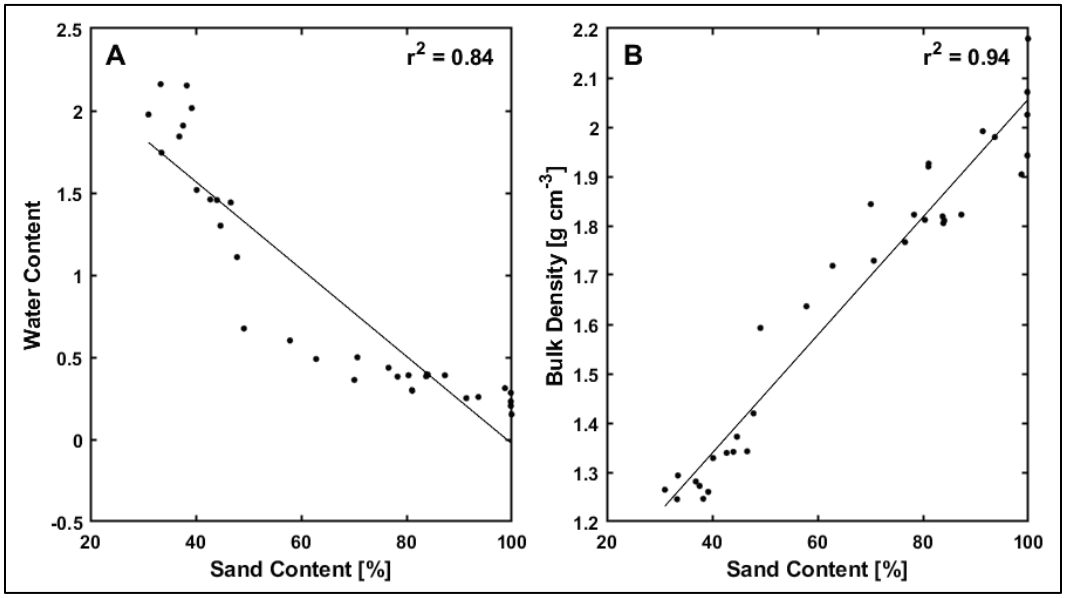

3.1.2 Plasticity index

Atterberg limit testing showed 21 of the 34 AIWW samples displayed plastic behavior that ranged in value from 8 to 151. A negative correlation was observed between sand content and plasticity (Figure 7; r^2=0.85) such that sediments with the lowest sand contents had the highest PI values. In general, when sand content of the AIWW sediments was >80%, a plasticity index was not measurable or reported with the exception of Florida Passage DM 102. For this sample, the PI value was 8 even though the sand content >80% (Table 2). PI results for all the other bottom materials are presented in Table 2.

Figure 7. Correlation of plasticity index with sand content.

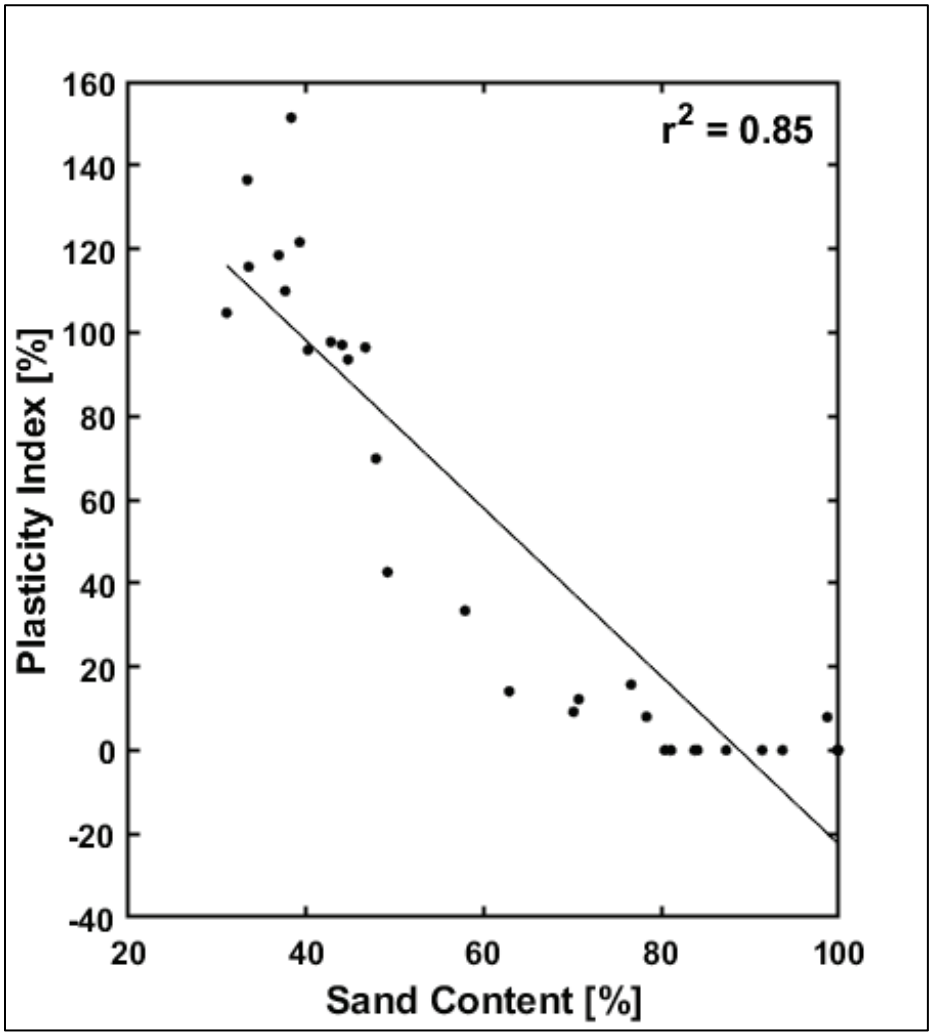

3.1.3 Organic content

Organic content measurements through LOI techniques were carried out and had values ranging from 0.2 to 9.1%. The highest LOI values occurred in samples with higher fine-grained sediment content. A complete summary of the LOI results is presented in Table 2.

3.1.4 Grain size

Grain size analysis performed on the samples showed that most of the sediments were sandy in texture, with 20 of the 34 having a sand content greater than 50% (Table 2), and none of the samples had sand content <30%. Despite a common sandy texture, the grain size distributions varied widely across the AIWW samples. The median grain size (D_{50}) of the sandy samples ranged from 110 μm to 788 μm, indicating that the sands within the AIWW spanned the Wentworth classification from very fine (63 – 125 μm) to coarse (500 – 1000 μm) sands. The 14 muddy (sand content <50%) samples within the AIWW were found to be dominated by silt with percentages ranging from 42% to 56%. Clay contents of these samples ranged from approximately 9% to 13%, with no sample in the AIWW having a clay content greater than approximately 13%.

Table 2 summarizes the percentage of sand, silt, and clay as well as the D_{50} of each AIWW sediment sample. Grain size distribution plots for the various locations in the SAS section of the AIWW are shown in Appendix A and are generally grouped based on sample number in chronological order. However, the five dry sieved samples (Sample numbers 12, 23, 25, 32, and 34) are grouped together since the distribution data are distinctively different than LDPSA samples.

Table 2. Physical properties of tested sediments. Shaded rows indicate non-cohesive sediments. * GSD obtained by dry sieve analysis. ** GSD obtained through combined LDPSA and sieve analysis.

Sample #	Sample Name	ρ (g/cm³)	*w*	PI	% LOI	D_{50} (μm)	% Sand	% Silt	% Clay
1	Center Ramshorn Creek	1.92	0.30	N/A	0.6	203	81.0	15.4	3.6
2	Southend Ramshorn Creek**	1.81	0.40	N/A	1.1	168	83.9	13.3	2.9
3	Walls Cut**	1.81	0.39	N/A	1.2	265	84.1	12.7	3.3
4	Northend Fields Cut**	1.77	0.44	16	1.5	209	76.6	19.2	4.2

Table 2. (cont.) Physical properties of tested sediments. Shaded rows indicate non-cohesive sediments. * GSD obtained by dry sieve analysis. ** GSD obtained through combined LDPSA and sieve analysis.

Sample #	Sample Name	ρ (g/cm³)	*w*	PI	% LOI	D_{50} (μm)	% Sand	% Silt	% Clay
5	Southend Fields Cut	1.59	0.67	43	3.7	69	49.2	42.1	8.7
6	Northend Elba Cut**	1.81	0.39	N/A	1.6	331	80.4	16.2	3.5
7	Southend Elba Cut	1.73	0.50	12	1.5	198	70.7	23.2	6.1
8	Vicinity DM 29	1.64	0.60	33	3.0	110	57.9	33.5	8.6
9	Northend Hell Gate DM 86	1.99	0.25	N/A	0.5	232	91.3	7.1	1.5
10	Hell Gate DM 89	1.34	1.44	96	5.7	61	46.6	44.4	9.0
11	Hell Gate DM 92	1.34	1.46	98	4.8	48	42.8	46.5	10.7
12	Florida Passage DM 102*	1.90	0.31	8	0.8	469	98.7	1.3	0
13	Creighton Narrows DM 155	1.29	1.74	116	5.4	26	33.5	53.4	13.1
14	Creighton Narrows DM 155A	1.27	1.91	110	5.4	33	37.6	50.5	11.9
15	Creighton Narrows DM 156	1.42	1.11	70	3.7	63	47.9	42.3	9.8
16	Doboy Sound DM 178	1.98	0.26	N/A	0.5	187	93.6	5.0	1.3
17	Rockdedundy @ DM 184	1.34	1.46	97	5.1	46	44.0	45.4	10.6
18	Rockdedundy DM 188**	1.93	0.30	N/A	1.0	388	81.1	15.8	3.2
19	Little Mud DM 190	1.26	2.02	122	7.1	37	39.3	50.4	10.4
20	Little Mud DM 192	1.26	1.98	105	6.4	23	31.0	55.9	13.1
21	Little Mud DM 194	1.37	1.30	94	5.4	52	44.7	45.9	9.4
22	Altamaha Sound DM 204-206	1.28	1.84	119	7.4	31	36.9	52.2	10.9
23	Altamaha Sound DM 208*	2.07	0.20	N/A	0.3	358	99.8	0.2	0
24	Altamaha Sound @ DM 211	1.82	0.39	N/A	1.2	385	87.3	10.6	2.1
25	Buttermilk Sound DM 218*	2.18	0.15	N/A	0.2	219	99.9	0.06	0
26	Buttermilk Sound DM 220	1.72	0.49	14	1.4	180	62.9	28.8	8.4
27	Buttermilk Sound DM 222	1.82	0.38	N/A	0.9	381	83.7	13.3	3.0

Table 2. (cont.) Physical properties of tested sediments. Shaded rows indicate non-cohesive sediments. * GSD obtained by dry sieve analysis. ** GSD obtained through combined LDPSA and sieve analysis.

Sample #	Sample Name	ρ (g/cm³)	*w*	PI	% LOI	D_{50} (μm)	% Sand	% Silt	% Clay
28	McKay River DM 234A	1.84	0.36	9	1.0	165	70.1	23.8	6.1
29	Jekyll Creek Northend	1.33	1.52	96	4.8	38	40.2	48.5	11.3
30	Jekyll Creek DM 13	1.25	2.16	137	9.1	27	33.4	54.5	12.2
31	Jekyll Creek DM 19	1.25	2.15	151	6.6	34	38.3	51.1	10.6
32	Cumberland Dividings DM 60*	1.94	0.28	N/A	0.3	788	99.8	0.2	0
33	Cumberland Sound RG	1.82	0.38	8	1.5	156	78.3	17.1	4.6
34	Cumberland Sound DM 75*	2.03	0.23	N/A	0.3	654	99.8	0.2	0

3.2 Erosion testing

A subset of sediments was selected from the 34 AIWW samples for erosion testing following initial geophysical property testing (Figure 1 and Table 3). The selected materials were screened such that the properties spanned both the geospatial and geophysical range of cohesive sediments from the AIWW. Based on prior research for predicting cohesiveness of sediments (e.g., Jacobs et al. 2011; Perkey et al. 2020b), samples with sand content >95% and those that had no measurable PI were determined to be non- or weakly cohesive and unlikely to produce robust aggregates. Therefore, these sediment types were excluded from erosion testing, and two cohesive samples with high (>75%) sand content and low PI (<20), two samples with moderate (~50%) sand content and PI <100, and two samples with low (<40%) sand content and PI >100 were chosen for erosion and aggregate testing (Figure 1 and Table 3).

Table 3. Cohesive AIWW samples selected for erosion and aggregate testing.

Sample #	Sample Name	% LOI	% Sand	% Silt	% Clay
4	Northend Fields Cut	1.5	76.6	19.2	4.2
10	Hell Gate DM 89	5.7	46.6	44.4	9.0
15	Creighton Narrows DM 156	3.7	47.9	42.3	9.8
22	Altamaha Sound DM 204-206	7.4	36.9	52.2	10.9
31	Jekyll Creek DM 19	6.6	38.3	51.1	10.6
33	Cumberland Sound RG	1.5	78.3	17.1	4.6

Analysis of cohesive sediment erosion data obtained from cores is inherently complex. Cohesive sediment erosion is sensitive to slight changes in bed density, deposit mineralogy, gas content, organic content, biological activity, and a host of other factors. In many cases, these factors change significantly at relatively small vertical scales. Consequently, measured cohesive sediment erosion rates from cores are notoriously noisy. To counter the large variance in measured erosion rates, erosion experiments are conducted in a manner to produce a large sample from which to derive statistically representative fits to various numerical erosion algorithms. To ensure high quality in the data analysis, data and associated experimental notes are evaluated to identify outliers in the dataset. Outliers are rejected based on comparisons between adjacent data points and experimental log notes.

Processing of FICS images for the calculation of particle size distribution requires the analyst to first review the collected images and define thresholds to identify and remove background objects within the FICS channel (such as scratches, stains, and streaks), air bubbles, and out of focus particles. During this process, any FICS videos that are unacceptable for particle size distribution analysis are also identified. For example, FICS videos may be excluded from analysis due to (1) poor lighting conditions as a result of heavy erosion and cloudy water in the flume or (2) from heavy bedload transport in which touching particles result in erroneously coarse size distributions. A total of 97 FICS videos were collected during the erosion testing of the six AIWW cores. Initial review of the videos showed that all the videos passed the quality control for size distribution analysis.

The results presented in the following are organized by sand content from highest to lowest. For each material, erosion data are presented followed by FICS and LDPSA GSD data (FICS) and bed aggregate production results. Observations made during erosion testing along with analysis of the Sedflume data showed that each sediment core displayed consistent erosion behavior with both depth and shear stress. Therefore, processed FICS video data were compiled to generate a FICS grain size distribution for each test core. Core descriptions including photographs are provided in Appendix B.

3.2.1 Cumberland Sound RG

Approximately 8.5 cm of sediment was eroded from the Cumberland Sound RG core over five cycles with applied shear stresses that ranged

from 2.2 to 6.4 Pa. The change in the rate of erosion for the applied shear stresses during the testing is presented in Figure 8. The data show a consistent behavior throughout the core and the best fit regression line indicated τ_{cr} =1.89 Pa, r^2= 0.94 (Figure 8). Prior to testing, a visual inspection of the core indicated a dark brown, homogeneous sediment throughout. Physical samples collected during erosion confirmed the uniform composition. Grain size results showed a near uniform 86% sand, 11% silt, and 3% clay composition with an average bed density of 1.78 g/cm^3 (Figure 9; Table 4).

The size distribution of eroded particles imaged by the FICS for the Cumberland Sound test material is presented in Figure 10 and was dominated by gravel sized particles (>2000 μm). Conversely, disaggregated GSDs of the material showed the coarsest grains to be on the order of 400 to 500 μm. This difference in the grain size distributions was supported by visual observations made during erosion testing which described aggregates being plucked from the bed with occasional bed failures generating larger aggregated clasts. Additionally, photos of the material retained on the 250 μm and 63 μm sieves during the collection of the flume effluent (Figure 11) indicated the presence of large, gravel-sized aggregates. Mass balance calculations revealed that 32 – 47% of the eroded mass was retained on the 250μm sieve. Results from wet sieving the disaggregated Cumberland Sound RG sediment found 6% of the material was >250 μm by mass. This suggests that 26% – 41% of the eroded Cumberland Sound RG material was in the form of macro-aggregates >250 μm. This agreed with the FICS distribution in which the majority of eroded material was in the form of gravel sized bed aggregates with a median (D_{50F}) diameter of ~4000 μm, a value more than 25× the disaggregated median grain size obtained from LDPSA (D_{50L}).

Figure 8. Erosion rate (E) versus shear stress (τ) for the Cumberland Sound RG core. The erosion testing data are indicated with colored circles. The color of the data point corresponds to the depth below the sediment-water interface. Regression lines and fit parameters are provided for the erosion data. The dashed lines represent the 95% confidence intervals in fit parameters.

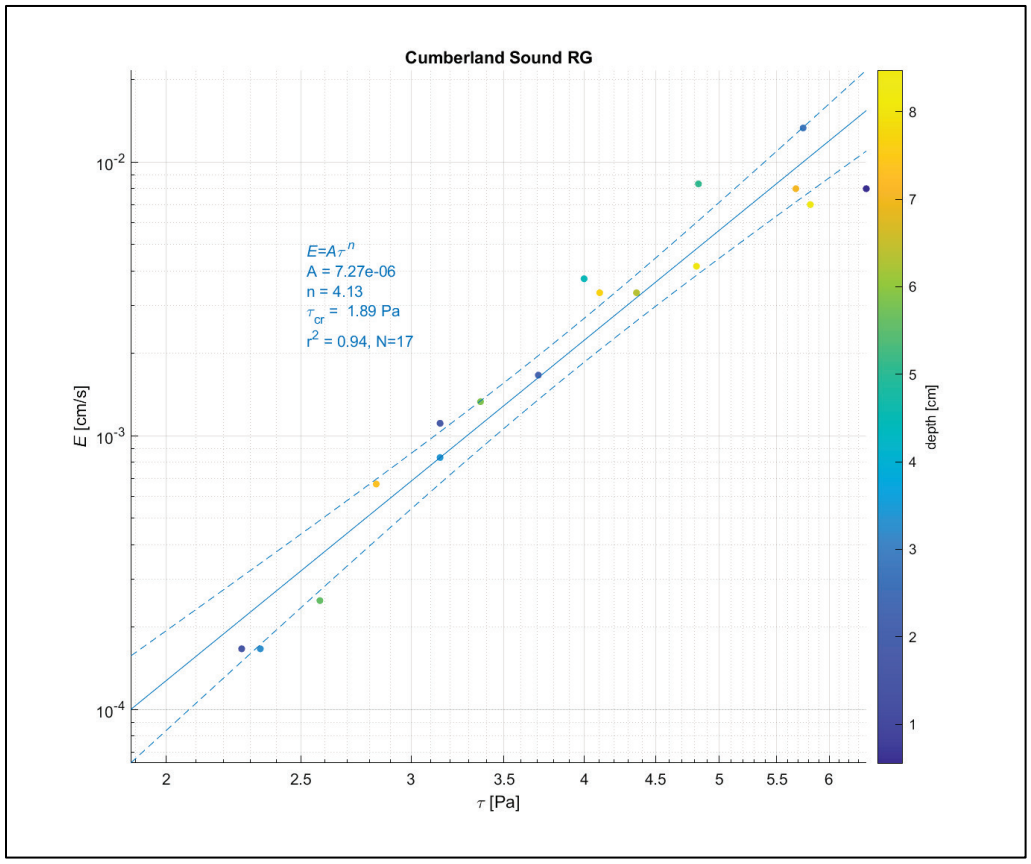

Figure 9. Grain size distributions for the Cumberland Sound RG sediment core physical samples collected during erosion testing.

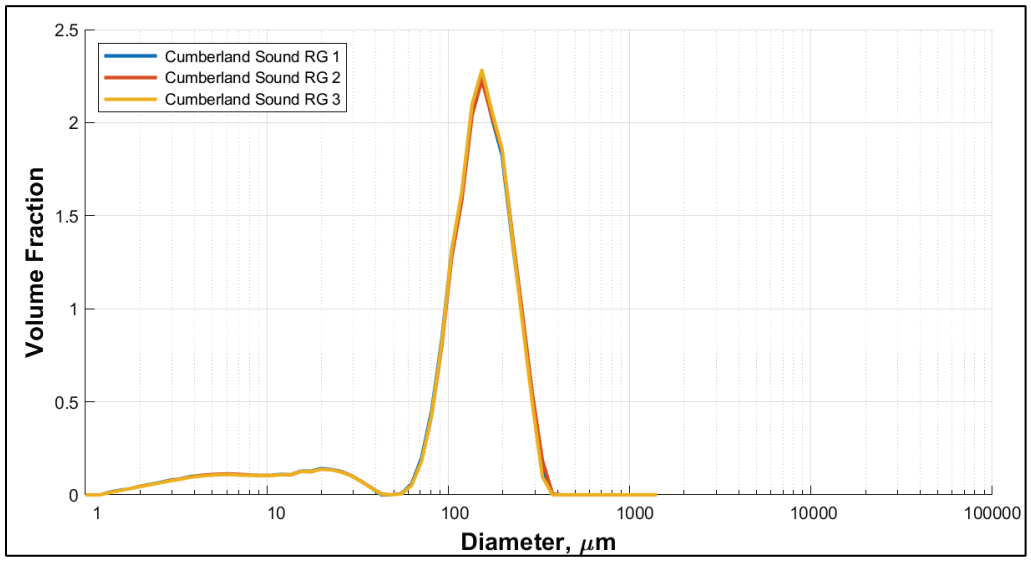

Figure 10. Grain size distribution for the Cumberland Sound RG sediment core from FICS data.

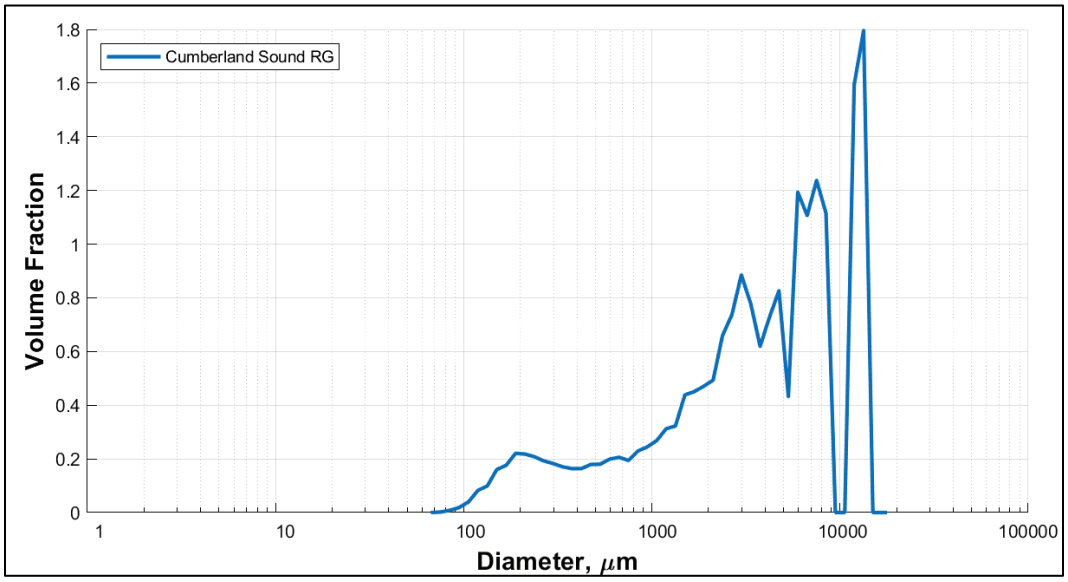

Figure 11. Photographs of Cumberland Sound RG sediment retained on 250 μm sieves (top) and 63 μm sieves (bottom).

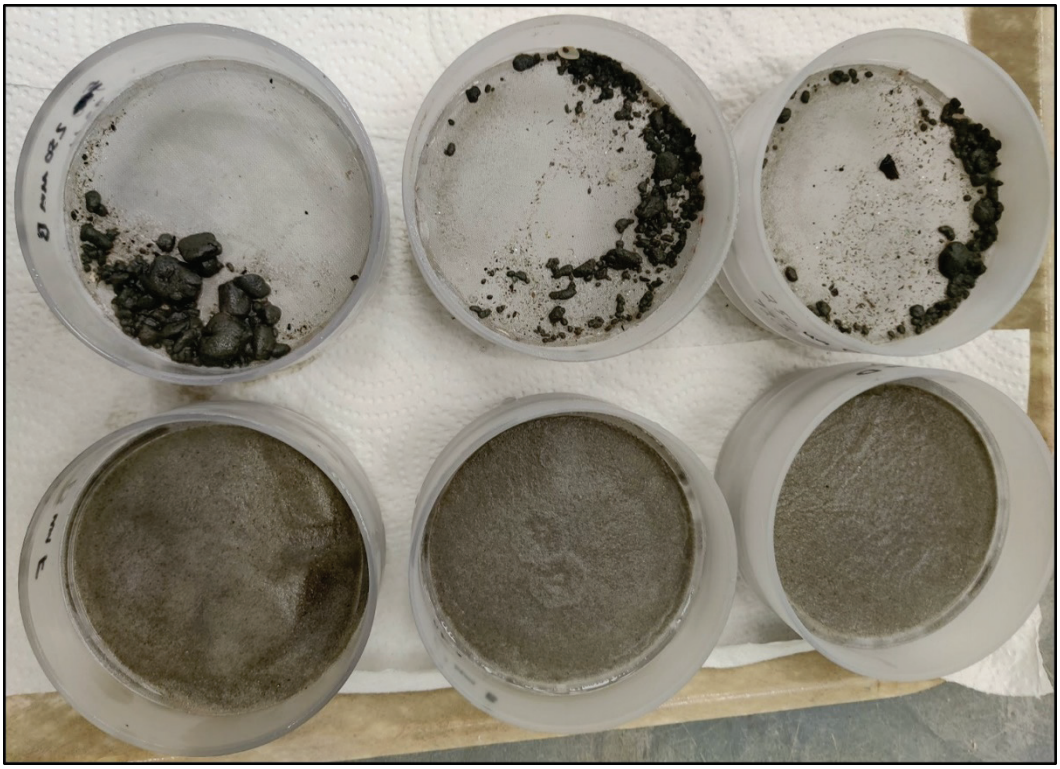

Table 4. Aggregate properties of eroded sediment, Cumberland Sound RG.

Sample #	Bulk Density (g/cm³)	D_{50L} (μm)	% Sand	% Silt	% Clay	D_{50F} (μm)	% >250 μm (Sedflume)	% >250 μm (Wet Sieve)	% Eroded Aggregate >250 μm
1	1.80	164	86.2	11.0	2.8	3950	33	6	27
2	1.76	166	86.3	11.0	2.7		32	6	26
3	1.78	164	86.5	10.8	2.7		47	6	41

3.2.2 Northend Fields Cut

Five repeated Sedflume cycles resulted in 10 cm of erosion in the Northend Fields Cut core. Erosion data plotting erosion rate versus applied shear stress are presented in Figure 12 and showed a consistent behavior throughout the core with a best fit regression line indicating τ_{cr} =1.67 Pa, r^2= 0.91 (Figure 12). Applied shear stresses during erosion testing ranged from approximately 2 Pa to 6.5 Pa. Grain size results of bed samples collected during erosion found the sand content varied slightly from approximately 70% to 74% while water content samples resulted in bulk densities ranging from 1.67 g/cm³ to 1.73 g/cm³ (Figure 13; Table 5). However, no consistent trends were observed in texture or bulk density with depth to indicate the presence of layering within the core.

FICS grain size distributions for Northend Fields Cut are presented in Figure 14. The FICS data showed a slight bi-modal distribution with abundant medium sand (250 – 500 μm) and gravel-sized particles accounting for approximately 20% and 43% of the eroded particles, respectively. The medium sand particles in the FICS distribution correspond with LDPSA grain size distributions that showed approximately 25% of the sediment was composed of medium sand. Erosion notes for this core consistently described both particle-by-particle and aggregate erosion. Photos of the material retained on the 250 μm sieves during collection of the Sedflume effluent showed both discrete sand particles and gravel-sized aggregates. The presence of these larger aggregates produced a D_{50F} of 1300μm, substantially larger than the median grain size of the LDPSA data that ranged from 157 μm to 172 μm (Table 5). However, the presence of these larger aggregated clasts was not consistently observed as noted by their abundance in sample collection 1 and 3, but limited presence in sample 2 (Figure 15; Table 5). Mass balance calculations revealed that 35% – 60% of the eroded mass was retained on the 250 μm sieve, compared to 33% retained when disaggregated and wet sieved. Calculations of the eroded mass occurring

as macro-aggregates ranged widely from 2% to 27% and indicated their inconsistency in production.

Figure 12. Erosion rate versus shear stress for the Northend Fields Cut core. The erosion testing data are indicated with colored circles. The color of the data point corresponds to the depth below the sediment-water interface. Regression lines and fit parameters are provided for the erosion data. The dashed lines represent the 95% confidence intervals in fit parameters.

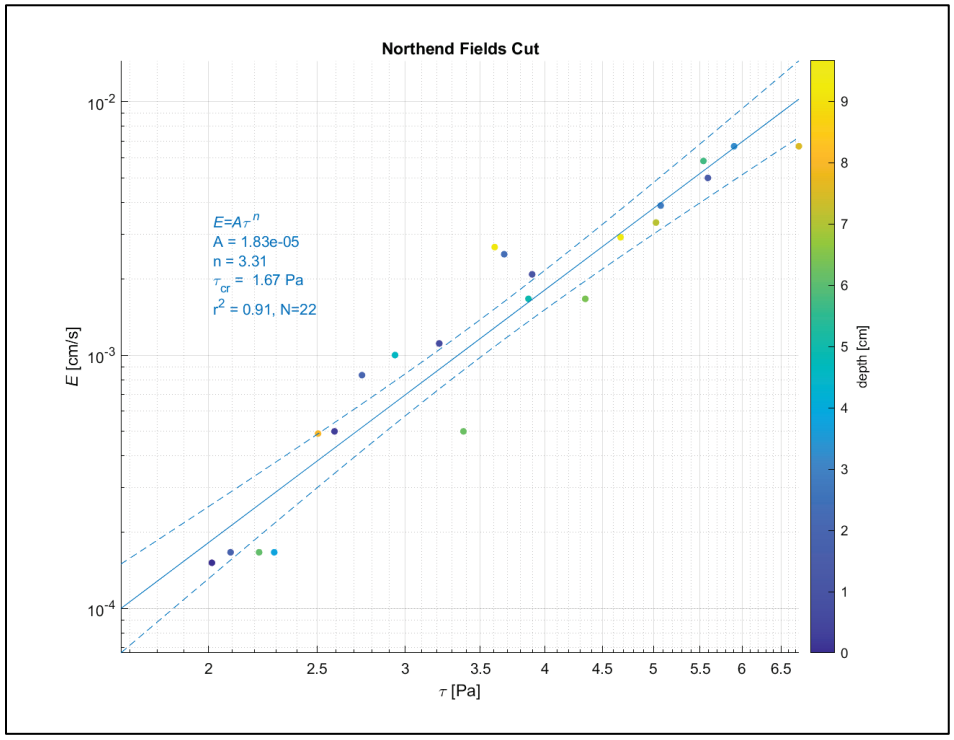

Figure 13. LDPSA grain size distributions for Northend Fields Cut sediment core physical samples.

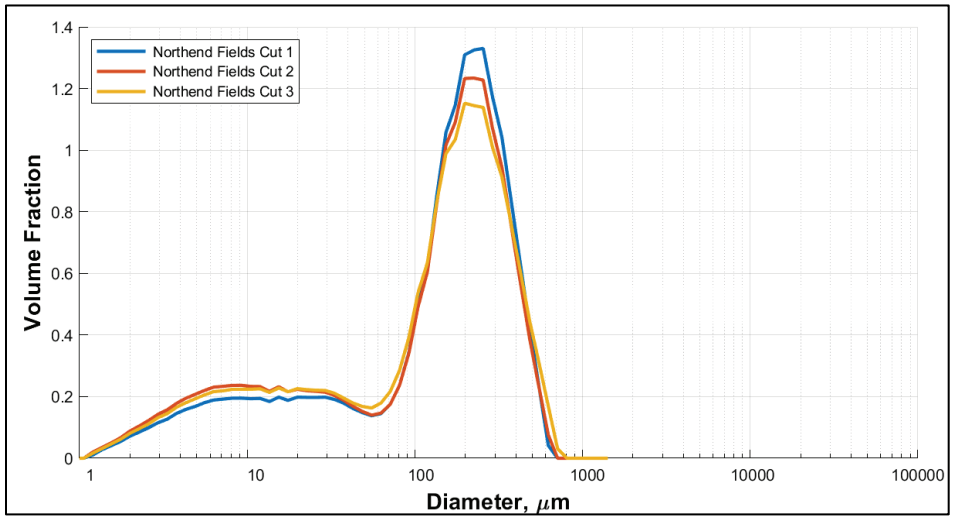

Figure 14. Grain size distribution for Northend Fields Cut sediment core FICS data.

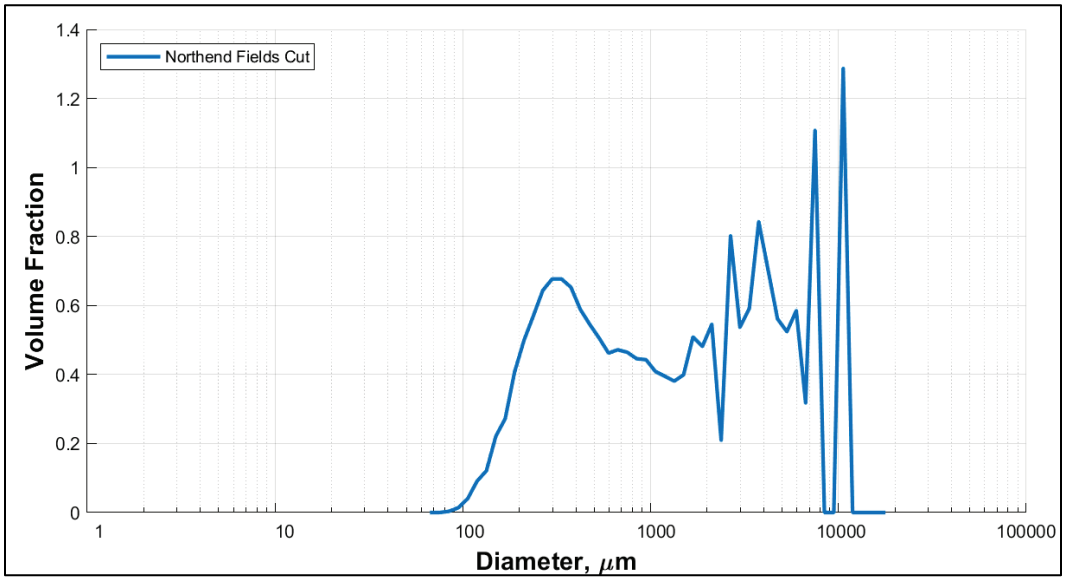

Figure 15. Photographs of Northend Fields Cut sediment retained on 250 μm sieves (top) and 63 μm sieves (bottom).

Table 5. Aggregate properties of eroded sediment, Northend Fields Cut.

Sample #	Bulk Density (g/cm³)	D_{50L} (μm)	% Sand	% Silt	% Clay	D_{50F} (μm)	% >250 μm (Sedflume)	% >250 μm (Wet Sieve)	% Eroded Aggregate >250 μm
1	1.73	196	74.1	21.7	4.3	1300	60	33	27
2	1.67	182	69.8	24.9	5.3		35	33	2
3	1.70	179	70.4	24.7	4.8		49	33	16

3.2.3 Creighton Narrows DM 156

Erosion testing of the Creighton Narrows DM 156 core involved approximately 6 cm of material across five repeated Sedflume cycles in which the applied shear stresses ranged from approximately 2.5 Pa to 7.5 Pa. Erosion data showed a consistent erosion rate with applied shear stress and the correlation predicted τ_{cr} to be 2.42 Pa (r^2= 0.76; Figure 16). Visual characterization of the core described a dark grey muddy material with notable shell hash and air bubbles dispersed throughout the core. Grain size results of physical samples show a uniform sediment texture with depth composed of approximately 40% sand, 50% silt, and 10% clay. The sediment was bi-modal with approximately 20% occurring as medium to coarse sand and >70% occurring as very fine sand (<125 μm) and mud (<63 μm). Note that these LDPSA results exclude any of the larger (>1000 μm) shell hash in the bed and thus are slightly skewed toward finer grains in comparison to the wet sieving method that showed 45% of the sediment mass was >250 μm. Bulk density samples showed a slight decrease from 1.49 g/cm³ at the surface to 1.43 g/cm³ at ~6 cm depth (Figure 17; Table 6).

In contrast to the LDPSA grain size, the FICS data showed more than 90% of imaged particles were >1000 μm (Figure 18). The FICS distribution yielded a median (D_{50F}) size that was approximately two orders of magnitude greater than that produced by laser diffraction (D_{50L}; Table 6). During testing of this core, it was noted that erosion occurred in the form of both particle-by-particle and aggregate erosion. Pictures of the material retained on the 250 μm sieves during the collection of the Sedflume effluent showed three types of sediment particles: (1) discrete sand grains, (2) shell hash, and (3) gravel sized aggregates. Again, the presence of these larger aggregated clasts was not consistently observed. The middle sample in Figure 19 showed more bed aggregates than the other two samples. Mass balance calculations revealed that 61% – 78% of the eroded mass was retained on the 250 μm sieve, compared to 45% that was retained when

the material was disaggregated and wet sieved. Thus, the eroded mass occurring as macro-aggregates varied from 16% to 33%.

Figure 16. Erosion rate versus shear stress for the Creighton Narrows DM 156 core. The erosion testing data are indicated with colored circles. The color of the data point corresponds to the depth below the sediment-water interface. Regression lines and fit parameters are provided for the erosion data. The dashed lines represent the 95% confidence intervals in fit parameters.

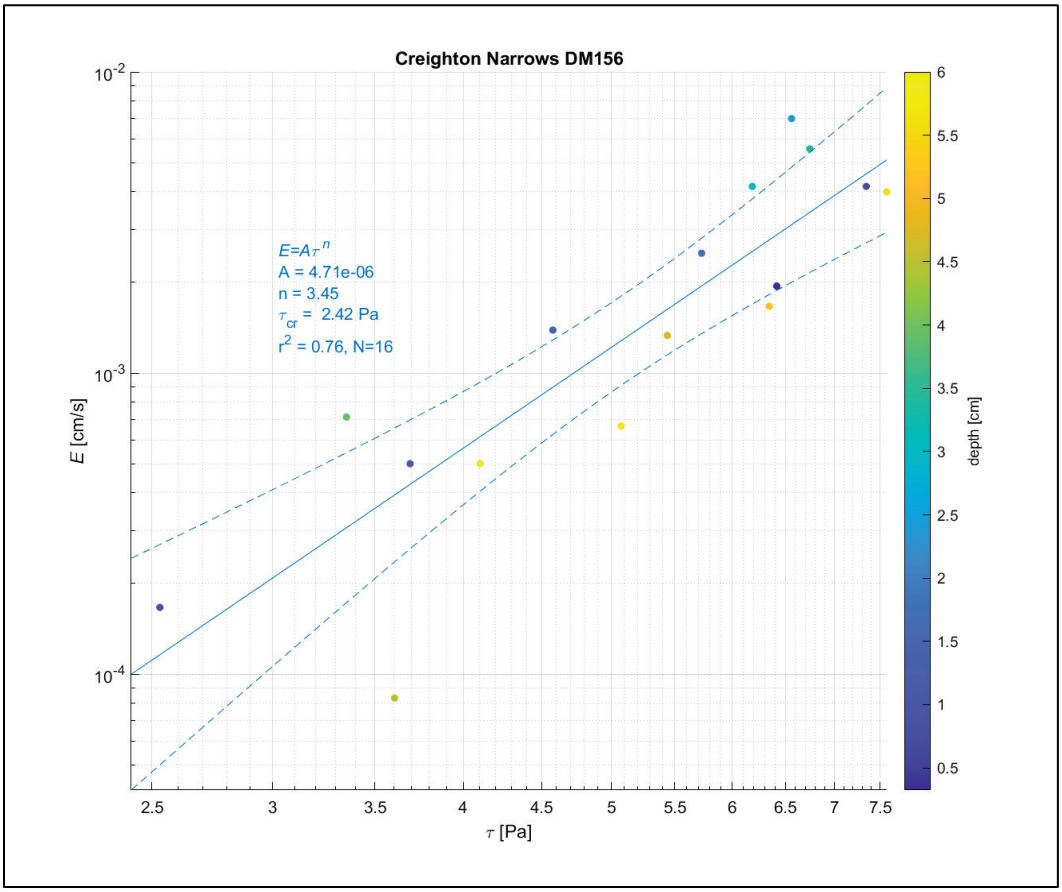

Figure 17. LDPSA grain size distributions for Creighton Narrows DM 156 sediment core physical samples.

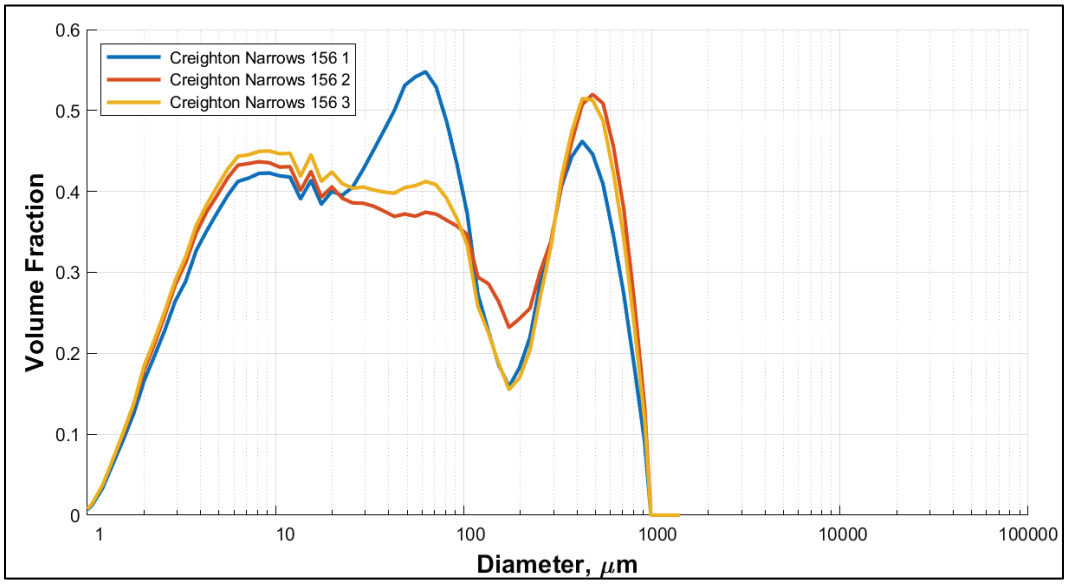

Figure 18. Grain size distribution for Creighton Narrows DM 156 sediment core FICS data.

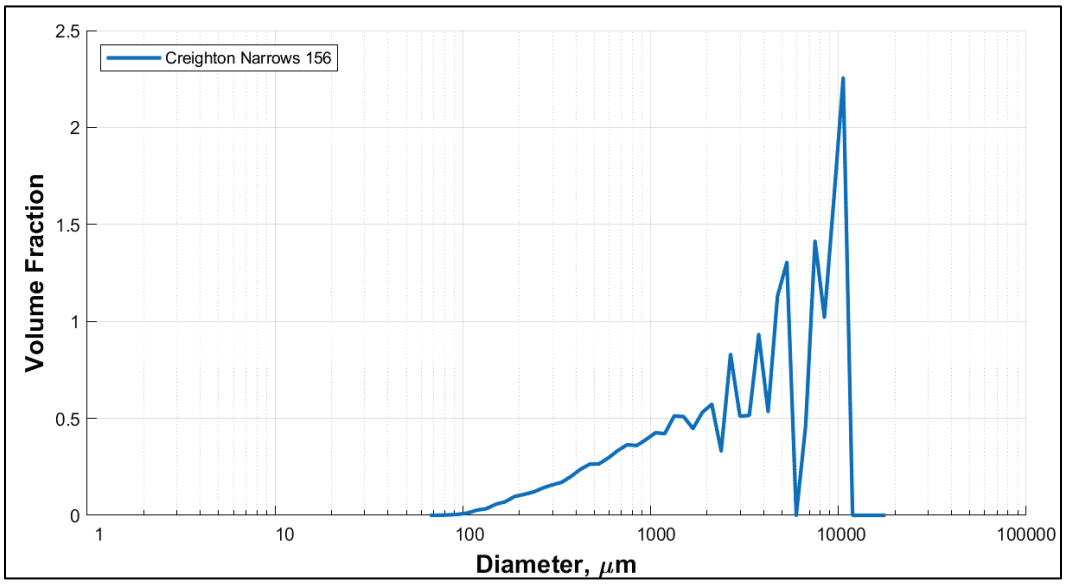

Figure 19. Photographs of Creighton Narrows DM 156 sediment retained on 250 μm sieves (top) and 63 μm sieves (bottom).

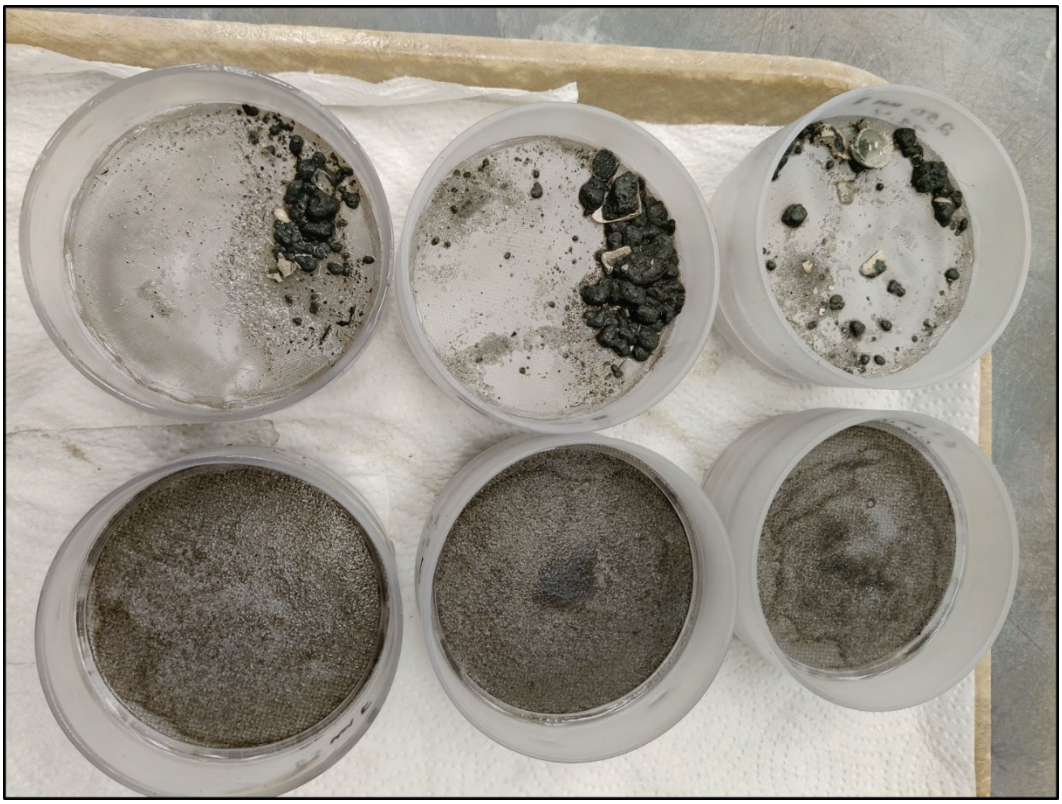

Table 6. Aggregate properties of eroded sediment, Creighton Narrows DM 156.

Sample #	Bulk Density (g/cm³)	D_{50L} (μm)	% Sand	% Silt	% Clay	D_{50F} (μm)	% >250 μm (Sedflume)	% >250 μm (Wet Sieve)	% Eroded Aggregate >250 μm
1	1.49	43.9	39.2	50.9	9.8	3860	61	45	16
2	1.46	42	41.6	47.8	10.6		78	6	33
3	1.43	38	39.2	50.0	10.8		69	6	24

3.2.4 Hell Gate DM 89

Prior to start of erosion testing of the Hell Gate DM 89 sediment core, visual descriptions noted air voids and cracks in the core. At the onset of testing, erosion behavior of the upper 5 – 8 cm was in the form of repeated bed failure. Below 8 cm depth to 12 cm, the sediment bed was more stable and less prone to large scale bed failure. Figure 20 presents the collected erosion data in a two-layer model in which the blue regression line represents the surface sediments (0 – 8 cm) that appeared to be significantly impacted by air voids and fractures resulting in bed failure. The τ_{cr} for the upper portion of the core was estimated to be 1.7 Pa

(r^2=0.82), though the 95% confidence bracket of this regression analysis was quite large due to the small number of data points (N=4). The orange regression line depicts the fit for the more intact sediment bed below 8 cm depth and predicted τ_{cr} to be 2.89 Pa (r^2= 0.7). Despite the two types of erosion behavior observed above and below 8 cm, grain size and bed density samples showed uniform texture (40% sand, 51% silt, 9% clay) and bulk density (1.34 g/cm^3) throughout the core (Figure 21; Table 7).

The GSD of the FICS data showed more than 70% of imaged particles were gravel sized aggregates >2000 μm (Figure 22) and generated a median particle size of approximately 4100 μm, which was two orders of magnitude greater than the average D_{50L} (46 μm; Table 6). Observations during erosion testing for this core described small to large bed aggregate erosion. The large aggregates were depicted in the photos of collected sediment from the flume outflow, Figure 23. Wet sieving of the disaggregated material showed that only 1% of the sediment was retained on a 250 μm sieve. Thus, indicating that nearly all the material captured on the 250 μm sieves in Figure 23 were macro-aggregates. Mass balance calculations suggested this to be 47% to 73% of the eroded sediment mass.

Figure 20. Erosion rate versus shear stress for the Hell Gate DM 89 core. The erosion testing data are indicated with colored circles. The color of the data point corresponds to the depth below the sediment-water interface. Regression lines and fit parameters are provided for the erosion data. The dashed lines represent the 95% confidence intervals in fit parameters.

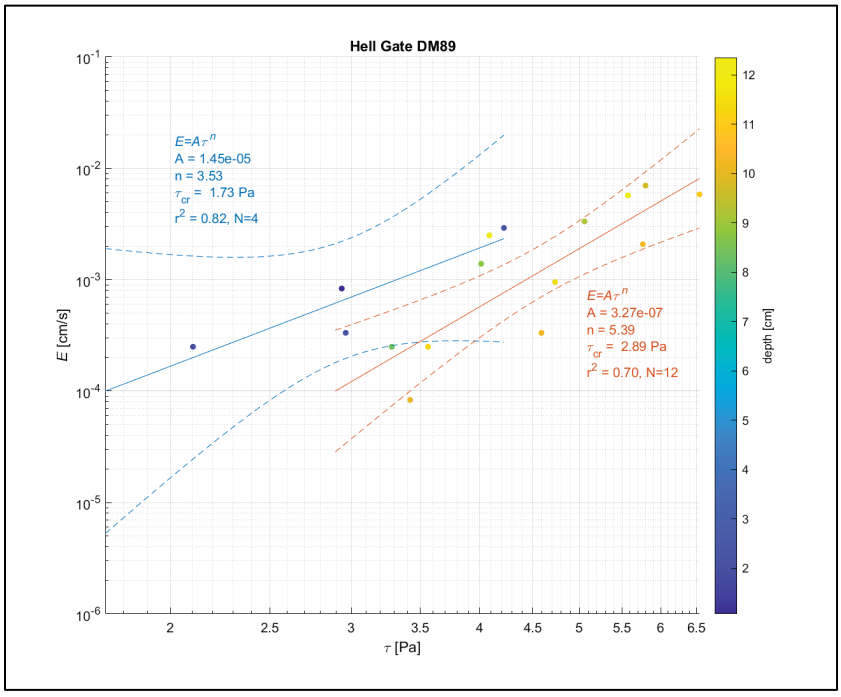

Figure 21. LDPSA grain size distributions for Hell Gate DM 89 sediment core physical samples.

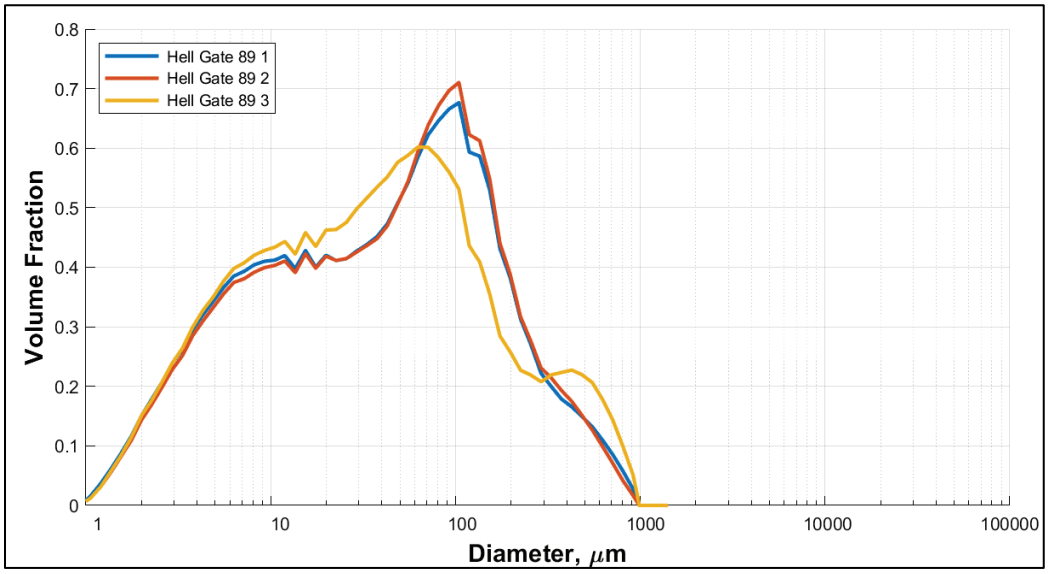

Figure 22. Grain size distribution for Hell Gate DM 89 sediment core FICS data.

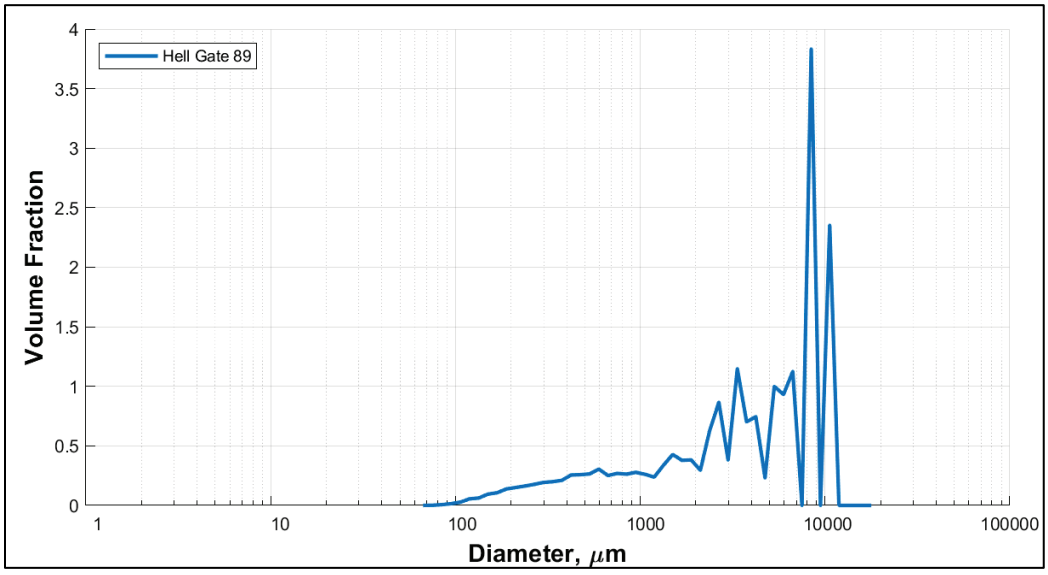

Figure 23. Photographs of Hell Gate DM 89 sediment retained on 250 μm sieves (top) and 63 μm sieves (bottom).

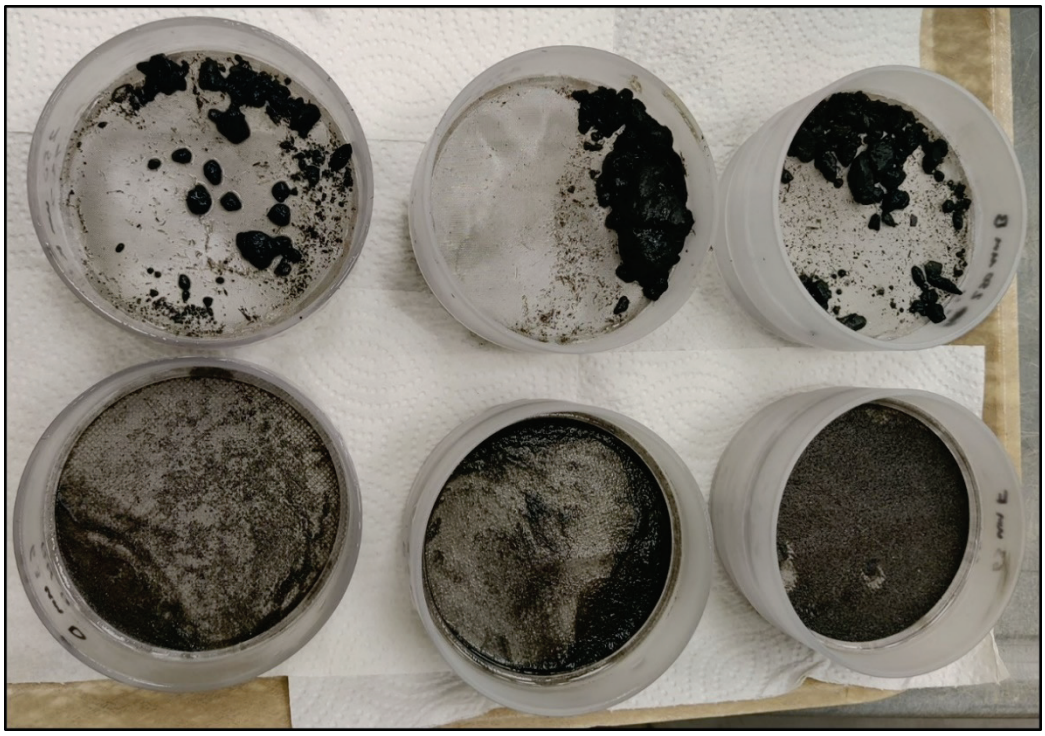

Table 7. Aggregate properties of eroded sediment, Hell Gate DM 89.

Sample #	Bulk Density (g/cm³)	D_{50L} (μm)	% Sand	% Silt	% Clay	D_{50F} (μm)	% >250 μm (Sedflume)	% >250 μm (Wet Sieve)	% Eroded Aggregate >250 μm
1	1.34	47.3	41.0	50.0	9.0	4118	62	1	61
2	1.36	49.9	42.1	49.3	8.6		74	6	73
3	1.34	40.8	36.6	54.5	9.0		48	6	47

3.2.5 Jekyll Creek DM 19

Approximately 10 cm of sediment was eroded from the Jekyll Creek DM 19 core over five cycles with shear stresses ranging from 2 Pa to 7 Pa. Erosion rate versus applied shear stress in Figure 24 showed a consistent trend throughout the core and predicted the τ_{cr} to be 2.1 Pa (r^2= 0.85). A large bed failure occurred at the start of the erosion testing that precluded the collection of data in the upper 2 cm of the core. As with the Hell Gate sediment, this failure was likely associated air voids that were noted in a visual examination of the core. Physical samples taken from the erosion surface showed that sand and silt content varied slightly down core; the sand content ranging from approximately 30% – 40% and silt from 50% –60%. Clay content and bulk density were more constant

with depth with values of 9% – 10% and 1.24 g/cm^3, respectively (Figure 25; Table 8).

Observed erosion behavior was characterized as aggregate erosion with periodic bed failures that produced large, aggregated clasts from the bed. The FICS data and photographs of the collected flume effluent support these observations. Size distribution of the FICS data showed more than 80% of imaged particles were gravel sized aggregates, and the D_{50F} was 3706 µm, approximately two orders of magnitude greater than the D_{50L} (Figure 26; Table 7). Wet sieving showed that only 2% of the disaggregated sediment was >250 µm. However, the three Sedflume effluent samples showed that 44% – 47% of the eroded sediment was retained on the 250 µm sieve (Figure 27; Table 8), meaning that 42% –45% of the eroded Jekyll Creek sediment was in the form of macro-aggregates.

Figure 24. Erosion rate versus shear stress for the Jekyll Creek DM 19 core. The erosion testing data are indicated with colored circles. The color of the data point corresponds to the depth below the sediment-water interface. Regression lines and fit parameters are provided for the erosion data. The dashed lines represent the 95% confidence intervals in fit parameters.

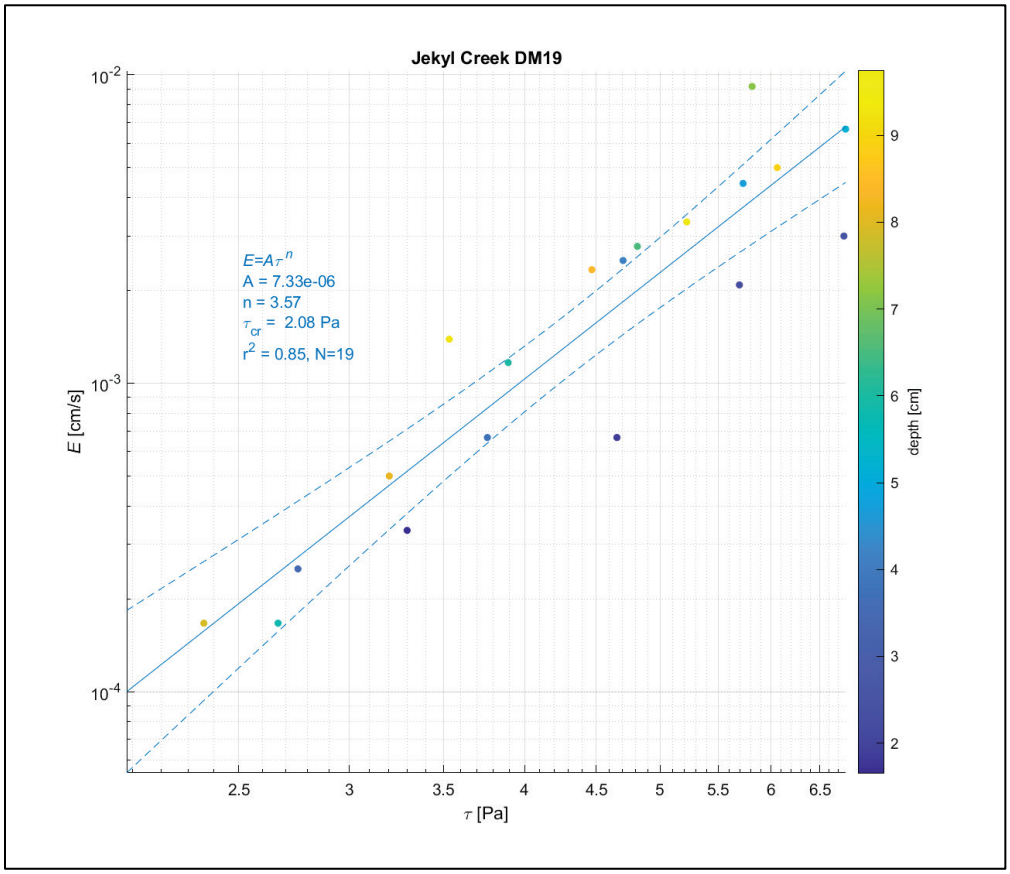

Figure 25. LDPSA grain size distributions for Jekyll Creek DM 19 sediment core physical samples.

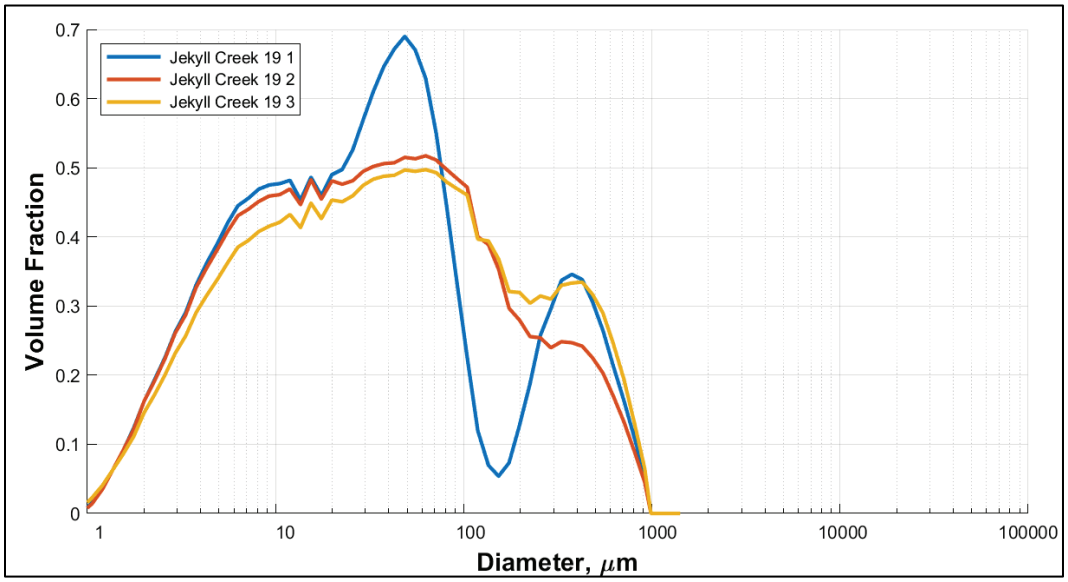

Figure 26. Grain size distribution for Jekyll Creek DM 19 sediment core FICS data.

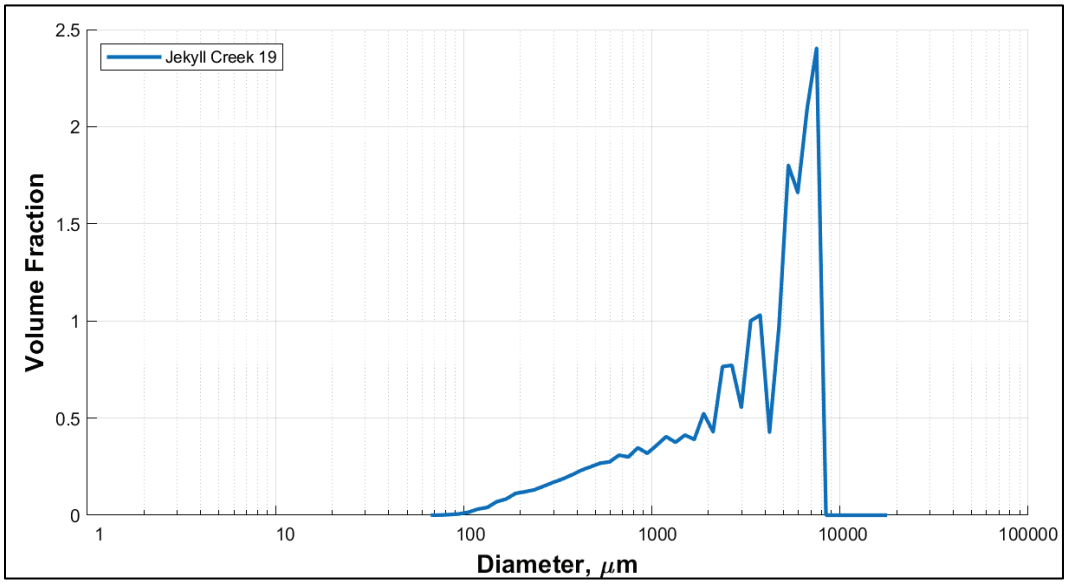

Figure 27. Photographs of Jekyll Creek DM 19 sediment retained on 250 μm sieves (top) and 63 μm sieves (bottom).

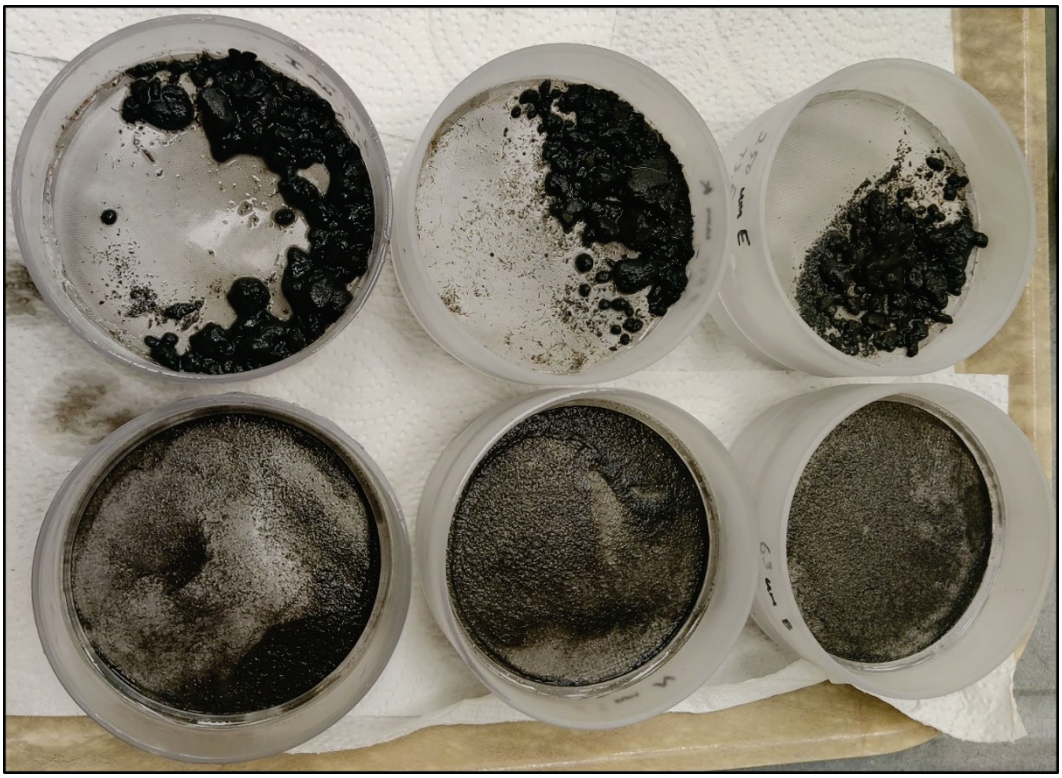

Table 8. Aggregate properties of eroded sediment, Jekyll Creek DM 19.

Sample #	Bulk Density (g/cm³)	D_{50L} (μm)	% Sand	% Silt	% Clay	D_{50F} (μm)	% >250 μm (Sedflume)	% >250 μm (Wet Sieve)	% Eroded Aggregate >250 μm
1	1.24	33.6	29.1	61.1	9.8	3706	44	1	43
2	1.23	36	35.2	55.1	9.7		46	6	45
3	1.24	43.6	39.8	51.4	8.9		47	6	46

3.2.6 Altamaha Sound DM 204-206

Sedflume evaluation of the Altamaha Sound DM 204-206 sediment core was conducted at shear stresses ranging from 1.5 Pa to 7.5 Pa that produced 14.5 cm of erosion. Reoccurring bed failures resulted in several centimeters of material being eroded at once and limited the number of erosion cycles that could be completed for the core. Multiple air voids noted in the visible examination of the core likely contributed to this behavior. As a result, only 3.5 erosion cycles were completed, but these data were sufficient (n=12) to predict a τ_{cr} of 1.8 Pa (r^2= 0.87) as shown in Figure 28. Grain size and bed density samples showed uniform texture

(35% sand, 50% silt, 10% clay) and bulk density (1.29 g/cm^3) throughout the core (Figure 29; Table 9).

The frequency of bed failures often produced a crumbled, uneven erosion surface that eroded almost exclusively in bed aggregates. The FICS size distribution showed more than 60% of imaged particles were gravel sized aggregates leading to a median particle size of approximately 2700 μm, which was approximately 80 times the D_{50L} (35 μm; Figure 30; Table 8). The number of macro-aggregates collected varied greatly for each of the three flume effluent samples (Figure 31). The mass balance calculations of the eroded sediment indicated that 20% – 69% of mass was in the form of macro-aggregates (Table 9).

Figure 28. Erosion rate versus shear stress for the Altamaha Sound DM 204-206 core. The erosion testing data are indicated with colored circles. The color of the data point corresponds to the depth below the sediment-water interface. Regression lines and fit parameters are provided for the erosion data. The dashed lines represent the 95% confidence intervals in fit parameters.

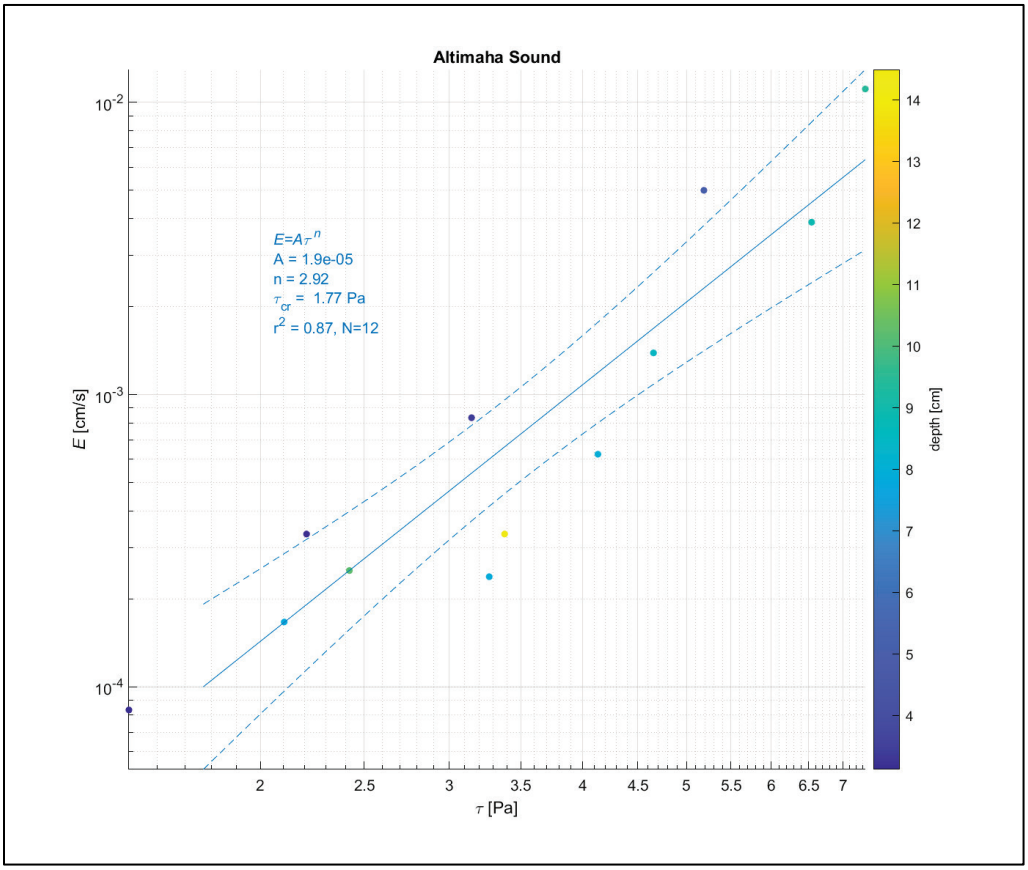

Figure 29. LDPSA grain size distributions for Altamaha Sound DM 204-206 sediment core physical samples.

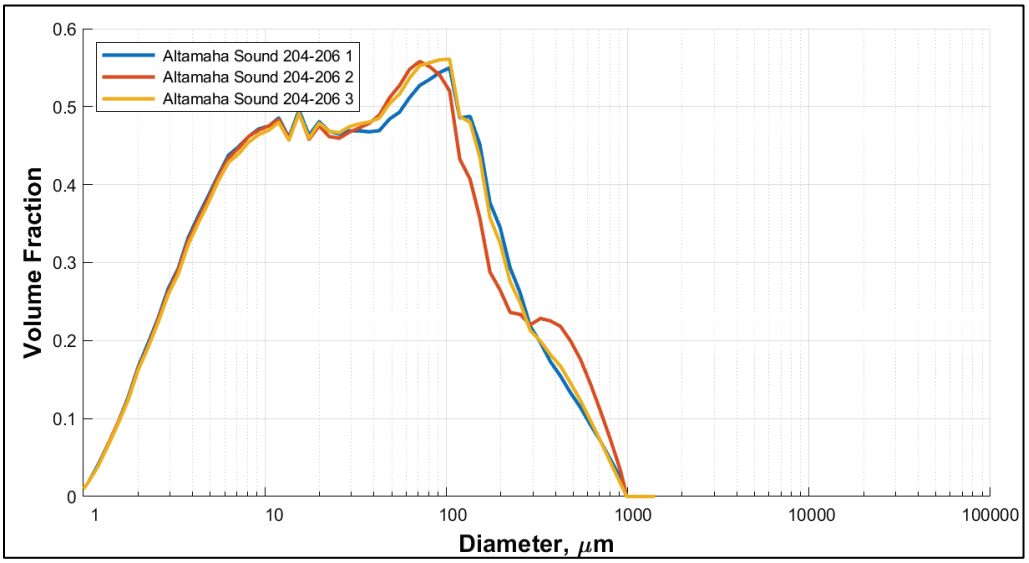

Figure 30. Grain size distribution for Altamaha Sound DM 204-206 sediment core FICS data.

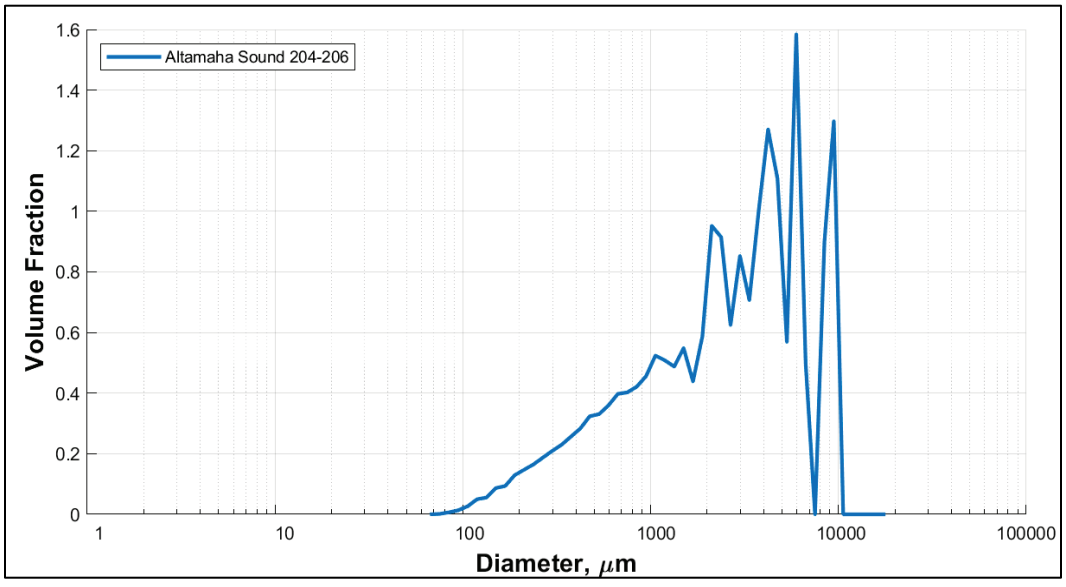

Figure 31. Photographs of Altamaha Sound DM 204-206 sediment retained on 250 μm sieves (top) and 63 μm sieves (bottom).

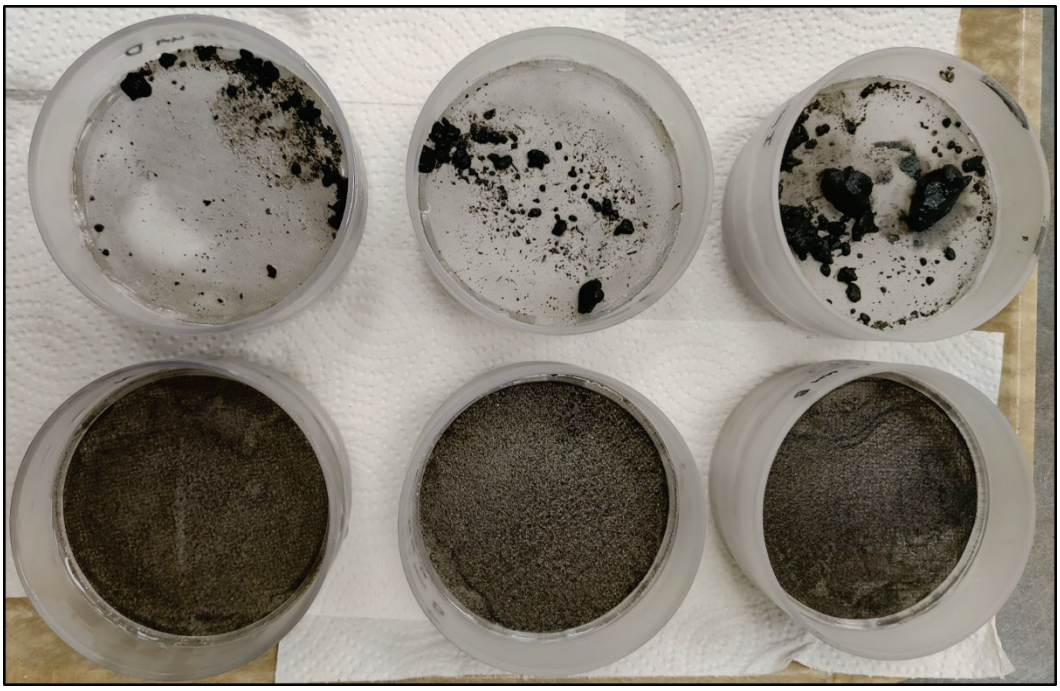

Table 9. Aggregate properties of eroded sediment, Altamaha Sound DM 204-206.

Sample #	Bulk Density (g/cm³)	D_{50L} (μm)	% Sand	% Silt	% Clay	D_{50F} (μm)	% >250 μm (Sedflume)	% >250 μm (Wet Sieve)	% Eroded Aggregate >250 μm
1	1.28	34.9	35.4	54.6	10.0	2712	71	2	69
2	1.29	35.5	35.1	55.0	9.9		35	6	33
3	1.29	36.1	35.6	54.7	9.7		22	6	20

3.3 Durability

Tumbling testing showed that all six of the samples showed break-up rates that closely followed an exponential model with $R^2 > 0.95$ (Table 9). In these models, the aggregated mass fraction >250 μm is related to tumbling time (t) through the abrasion rate (δ) shown in Equation 3:

$$F_{Ma>250} = Ae^{-\delta t} \quad (3)$$

While aggregate abrasion closely matched an exponential model, the deterioration rates varied substantially, as evident by the range in δ in Table 9. The Northend Fields Cut material was found to be the weakest material, with an aggregate abrasion rate of 0.209/min and no macro-aggregated mass remaining after 20 min of tumbling. The five other test

samples had measurable macro-aggregated mass in the tumbler after 20 min, a value equivalent to approximately 200 m of rolling as bedload transport. Material from Cumberland Sound RG and Creighton Narrows DM 156 had similar abrasion rates of approximately 0.1/min and $F_{Ma>250}$ values of 0.09 and 0.12, respectively, after 20 min of tumbling. Altamaha Sound DM 204-206, Hell Gate DM 89, and Jekyll Creek DM 19 had the most resilient aggregates with δ values of 0.057/min, 0.053/min, and 0.042/min, respectively (Figure 32, Table 10). Aggregates from Jekyll Creek were the most robust with $F_{Ma>250} = 0.42$ after 20 min of tumbling while Altamaha Sound and Hell Gate $F_{Ma>250}$ values were both approximately 0.3 (Figure 32).

Figure 32. Aggregate durability plots of AIWW erosion core samples. Dotted lines indicate exponential fits.

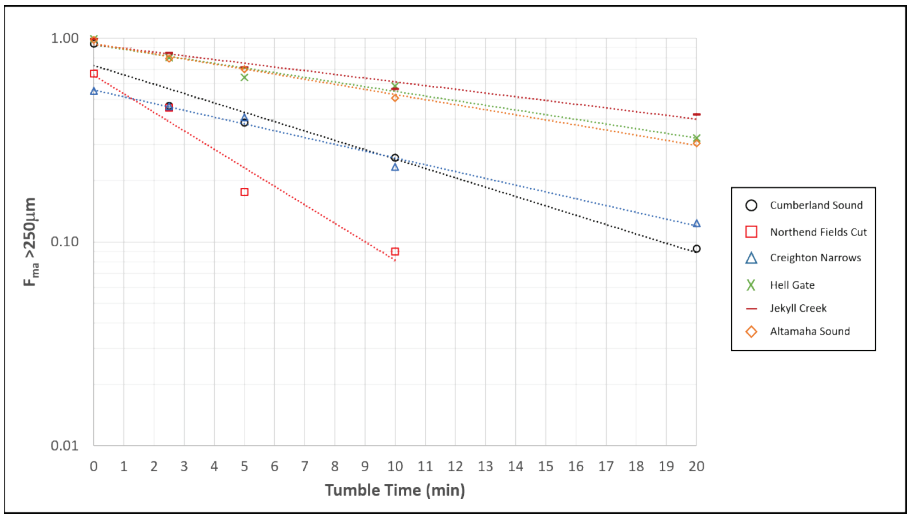

Table 10. Aggregate durability tumbling results. Bulk density of tumbled aggregates (ρ) and tumbling abrasion rate (δ) are presented with the r^2 values of the regression model fit. The asterisk (*) indicates samples with reduced w values for aggregate testing.

Sample Name	ρ (g/cm³)	δ (1/min)	r^2
Cumberland Sound RG	1.78	0.106	0.961
Northend Fields Cut	1.70	0.209	0.956
Creighton Narrows DM 156	1.46	0.077	0.988
Hell Gate DM 89	1.35	0.053	0.973
Jekyll Creek DM 19	1.29*	0.042	0.966
Altamaha Sound DM 204-206	1.34*	0.057	0.994

4 Summary and Conclusions

To evaluate potential BUDM applications for channel sediments from portions of the AIWW maintained by SAS, 34 vibracore borings spanning the area from Beaufort County, South Carolina, to Camden County, Georgia, were collected and analyzed for commonly measured physical properties (grain size, density, water content, plasticity, and organic content). Seeking to use locally sourced dredged material containing fine sediment (<63 μm) for bird island construction and wetland nourishment, SAS had a particular interest in evaluating if placed material would contain mud aggregates that are less likely to be dispersed throughout the system. In addition to investigating the likelihood of each of the sediments to produce aggregates, the material was tested to determine how resistant to erosion these sediments might be after placement.

Previous studies have linked plasticity and clay content to cohesive behavior in sediments (e.g., van Ledden et al. 2004; Jacobs et al. 2011; Wu et al. 2018; Perkey et al. 2020b,c) and demonstrated that small amounts of clay (3% – 5%) can produce cohesive behavior. Grain size analysis of the sediments revealed that 20 of the 34 samples were sandy in texture (sand content >50%) while 14 were muddy (sand content <50%). However, 14 of the 20 sandy sediment samples examined displayed no plasticity and/or had clay contents less than 3%. This suggests that these sediments would display little to no cohesive behavior and would be unlikely to produce macro-aggregates (Table 2). Depending on local regulatory policies regarding fines content and sediment color, these non-cohesive, high sand content sediment samples could be appropriate for beach nourishment, island/berm construction, or another similar BUDM applications. Assessment of the erodibility of these sediments would best be determined through non-cohesive methods such as the modified shields curve (Soulsby and Whitehouse 1997).

The remaining 20 sediments in this study were classified as cohesive and a subset of 6 of these samples were selected for further erosion and macro-aggregate (>250 μm) production. These samples were chosen to span both the range in PI and sand content and the geospatial study area (Table 3). Test cores of these sediments were prepared and allowed to self-weight consolidate for 30 days prior to erosion testing with the Sedflume and FICS. Regression analysis of the erosion data for the test materials showed critical shear stress values ranged from approximately 1.7 Pa to 2.9 Pa.

These values suggest that these sediments would be quite resistant to erosion following placement and a short consolidation period. Many of the potential placement areas for the AIWW sediments are low-energy wetland/tidal flat environments that are rarely exposed to bottom stresses >1 Pa outside of storm events (Seime et al. 2002; Blanto et al. 2003; Christiansen et al. 2000; Shi et al. 2012; Verney et al. 2006; Fall et al. 2021). Investigations to evaluate the flow velocities likely to occur at the placement site would be needed to fully determine the transport potential of the placed dredged material, but the τ_{cr} values measured in this study are likely to exceed typical shear stresses observed in the coastal wetlands of South Carolina and Georgia. In these environments, the macro-aggregated clasts may have limited mobility and thus increase sedimentation and accumulation at the placement area.

Sediment samples collected from the outflow of the Sedflume during erosion testing, along with FICS grain size distributions, indicated that macro-aggregates (>250 μm) were commonly produced during the erosion of each core. Comparison of the median FICS grain size (D_{50F}) to that of the disaggregated bed material measured via LDPSA (D_{50L}) found that the eroded aggregates were one to two orders of magnitude larger than the primary particles in the sediment bed. Additionally, the recorded presence of these aggregates under high shear stress conditions in the flume lends evidence to suggest that similar high shear events associated with dredging operations would also produce aggregated clasts.

The abundance of these aggregates varied considerably among the test materials. Differences in the measured mass of macro-aggregates eroded was on the order of 20% for five of the six test materials. Despite this variability, each core had at least one sample that showed ≥20% of the eroded mass occurred as macro-aggregates. Thus, the data generated in this study suggest that aggregated mud clasts should be anticipated to occur in sediment beds composed of the AIWW cohesive materials.

Durability testing of aggregate cubes composed of the six AIWW test materials found these aggregates to be robust and resilient to abrasion likely to be encountered during bed load transport. The Northend Fields Cut sediment generated the weakest aggregates; ~10% of its macro-aggregate mass was maintained after 10 min of tumbling. However, the tumbler experiments suggested that aggregates approximately 1 cm in diameter were robust enough to withstand bed load transport of ~100 m of linear distance.

The remaining five samples had macro-aggregate mass remaining after 20 min of tumbling (~200 m of linear distance). In particular, aggregates created from Hell Gate DN 89, Jekyll Creek DM 19, and Altamaha Sound DM 204-206 sediments were the most robust with greater than 30% of their mass persisting after 20 min. BUDM projects constructed with these materials should anticipate the presence of large robust aggregates. Thus, while the fines content (<63 μm) of these sediments is in the range of 30% to 70%, the physical properties allow these fines to be packaged in larger, robust clasts. Such features would be viewed as positives for BUDM projects seeking to build berms/islands or raise elevation within a specific location. Conversely, if the goal of the BUDM project was to rely on local waves and currents to disperse the fine-grained sediment in a far field nourishing event throughout the tidal flat or wetland, then the occurrence of macro-aggregated clasts would hinder the desired outcome.

References

ASTM (ASTM International) D2216-19. 2019. *Standard Test Methods for Laboratory Determination of Water (Moisture) Content of Soil and Rock by Mass*. West Conshohocken, PA: ASTM International.

ASTM D2974-14. 2014. *Standard Test Methods for Moisture, Ash, and Organic Matter of Peat and Other Organic Soils*. West Conshohocken, PA: ASTM International.

ASTM D4318-05. 2015. *Standard Test Methods for Liquid Limit, Plastic Limit and Plasticity Index of Soils*. West Conshohocken, PA: ASTM International.

ASTM D4644-87. 1998. *Standard Test Method for Slake Durability of Shales and Similar Weak Rocks*. West Conshohocken, PA: ASTM International.

ASTM D6913M-17. 2017. *Standard test methods for particle-size distribution (gradation) of soils using sieve analysis*. West Conshohocken, PA: ASTM International.

Blanton, J. O., H. Seim, C. Alexander, J. Amft, and G. Kineke. 2003. "Transport of Salt and Suspended Sediments in a Curving Channel of a Coastal Plain Estuary: Satilla River, GA." *Estuarine, Coastal and Shelf Science* 57(5–6): 993–1006.

Christiansen, T., P. L. Wiberg, and T. G. Milligan. 2000. "Flow and Sediment Transport on a Tidal Salt Marsh Surface." *Estuarine, Coastal and Shelf Science* 50(3): 315–331.

Fall, K. A, D. W. Perkey, and S. J. Smith. 2020. *Characterization of Eroded Mud Aggregates with the Flume Imaging Camera System (FICS) and Its Added Value to Sediment Management Projects*. ERDC/TN DOER-D22. Vicksburg, MS: US Army Engineer Research and Development Center.

Fall, K. A., D. W. Perkey, Z. J. Tyler, and T. W. Welp. 2021. *field Measurement and Monitoring of Hydrodynamic and Suspended Sediment within the Seven Mile Island Innovation Laboratory, New Jersey*. ERDC/CHL TR-21-9. Vicksburg, MS: US Army Engineer Research and Development Center.

Jacobs, W., P. Le Hir, W. Van Kesteren, and P. Cann. 2011. "Erosion Threshold of Sand-Mud Mixtures." *Cont. Shelf Res.* 31(10) (S14–S25). doi:10.1016/j.csr.2010.05.012.

Jepsen, R., J. Roberts, and J. Gailani. 2010. "Effects of Bed Load and Suspended Load on Separation of Sands and Fines in Mixed Sediment." *J. Waterw. Port, Coast. Ocean Eng*. 136(6): 319–326. https://doi.org/10.1061/(ASCE)WW.1943-5460.0000054.

McNeil, J., C. Taylor, and W. Lick. 1996. "Measurements of Erosion of Undisturbed Bottom Sediments with Depth." *Journal of Hydraulic Engineering* 122(6): 316–324.

Perkey, D. W., S. J. Smith, K. A. Fall, G. M. Massey, C. T. Friedrichs, and E. M. Hicks. 2020a. "Impacts of Muddy Bed Aggregates on Sediment Transport and Management in the tidal James River, VA." *Journal of Waterway, Port, Coastal, and Ocean Engineering*. DOI: 10.1061/(ASCE)WW.1943-5460.0000578

Perkey, D. W., S. J. Smith, and A. M. Priestas. 2020b. *Erosion Thresholds and Rates for Sand-Mud Mixtures*. ERDC/CHL TR-20-13. Vicksburg, MS: US Army Engineer Research and Development Center.

Perkey, D. W., K. A. Fall, and S. J. Smith. 2020c. *Physical Factors That Influence Muddy Bed Aggregate Production, Size, and Durability*. ERDC/CHL TR-20-19. Vicksburg, MS: US Army Engineer Research and Development Center.

Salehi, M. H., O. Hashemi Beni, H. Beigi Harchegani, I. Esfandiarpour Borujeni, and H. R. Motaghian. 2011. "Refining Soil Organic Matter Determination by Loss-on-Ignition." *Pedosphere* 21(4): 473–482.

Schumacher, B. A. 2002. "Methods for the Determination of Total Organic Carbon (TOC) in Soils and Sediments." 1–23.

Seim, H. E., J. O. Blanton, and T. Gross. 2002. "Direct Stress Measurements in a Shallow, Sinuous Estuary." *Continental Shelf Research* 22(11–13): 565–1578.

Shi, B. W., S. L. Yang, Y. P. Wang, T. J. Bouma, and Q. Zhu. 2012. "Relating Accretion and Erosion at an Exposed Tidal Wetland to the Bottom Shear Stress Of Combined Current–Wave Action." *Geomorphology* 138(1): 380–389.

Smith, S. J., and C. T. Friedrichs. 2011. "Size and Settling Velocities of Cohesive Flocs and Suspended Sediment Aggregates in a Trailing Suction Hopper Dredge Plume." *Continental Shelf Research* 31(10): S50–S63. doi:10.1016/j.csr.2010.04.002.

Soulsby, R. L., and R. Whitehouse. 1997. "Threshold of Sediment Motion in Coastal Environments." In *Proc., Pacific Coasts and Ports '97 Conf.* 149–154 Christchurch, New Zealand: Univ. of Canterbury.

Van Ledden, M., W. G. M. Van Kesteren, and J. C. Winterwerp. 2004. "A Conceptual Framework for the Erosion Behaviour of Sand-Mud Mixtures." *Continental Shelf Research*. 24(1): 1–11. https://doi.org/10.1016/j.csr.2003.09.002.

Verney, R., J. C. Brun-Cottan, R. Lafite, J. Deloffre, and J. A. Taylor. 2006. "Tidally Induced Shear Stress Variability above Intertidal Mudflats in the Macrotidal Seine Estuary." *Estuaries and Coasts* 29(4): 653–664.

Wentworth, C. K. 1929. "Method of Computing Mechanical Composition Types in Sediments." *Bulletin of the Geological Society of America* 40(4): 771–790.

Wu, W., C. Perera, S. J. Smith, and A. Sanchez. 2018. "Critical Shear Stress for Erosion of Sand and Mud Mixtures." *Journal of Hydraulic Research* 56(1): 96–110.

Appendix A: Grain Size Distributions of AIWW Vibracore Samples

This appendix presents figures showing the grain size distribution plots of the 34 coring borings collected from the AIWW (Figures A-1 through A-9).

Figure A-1. Grain size distribution using equivalent spherical diameter (esd; μm) for boring samples at center Ramshorn Creek (1), South end Ramshorn Creek (2), and Walls Cut (3).

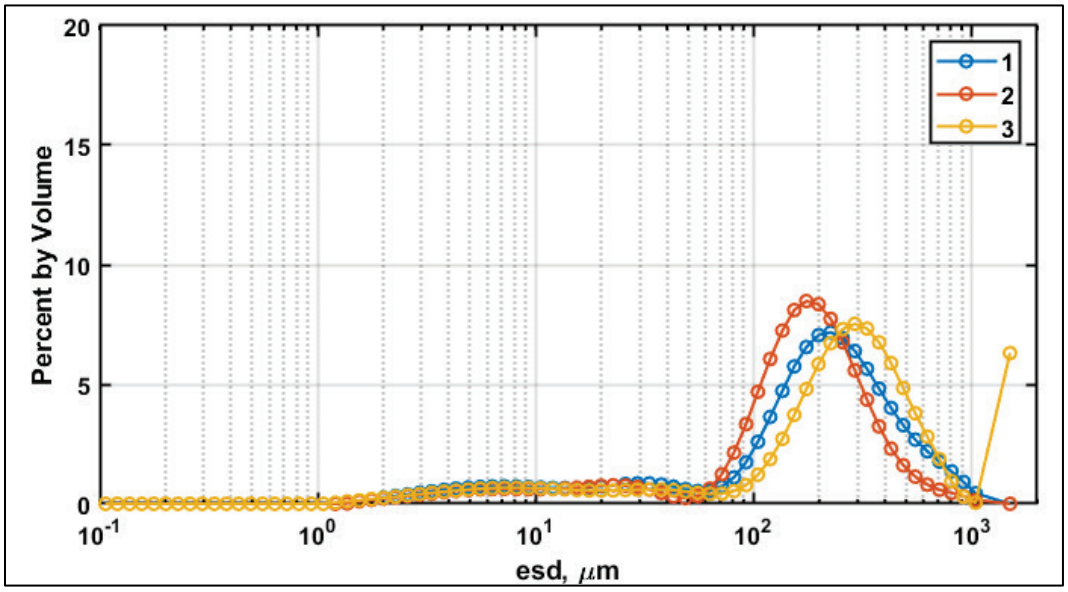

Figure A-2. Grain size distribution using equivalent spherical diameter (esd; μm) for boring samples at Fields Cut at the north end (4), and south end (5), Elba Cut at the north end (6) and south end (7), and Vicinity DM 29 (8).

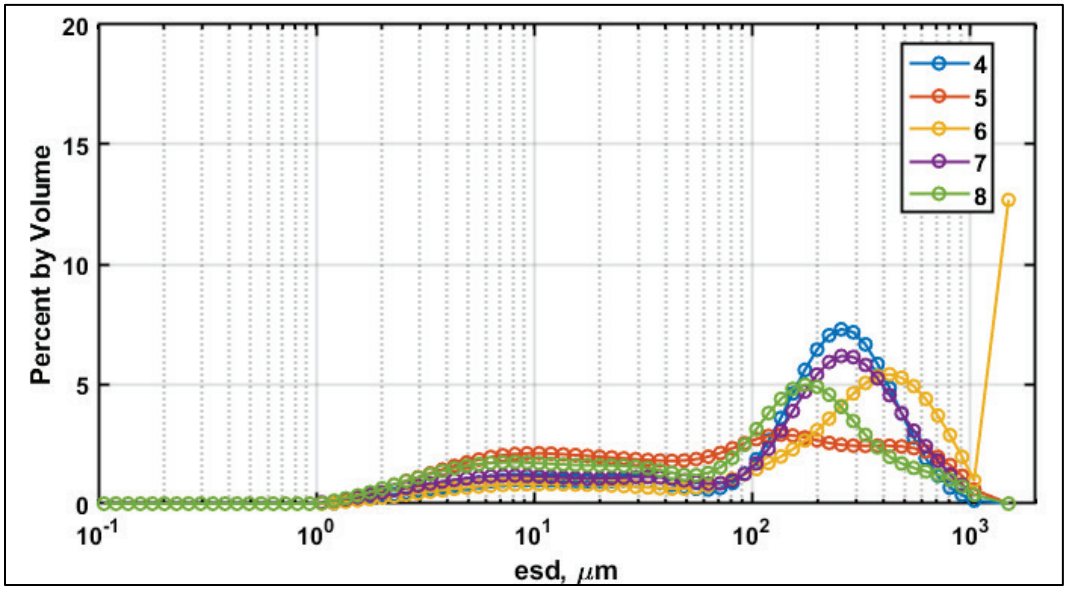

Figure A-3. Grain size distribution using equivalent spherical diameter (esd; μm) for boring samples at Hells Gate for the north end (9), DM 89 (10), and DM 92 (11).

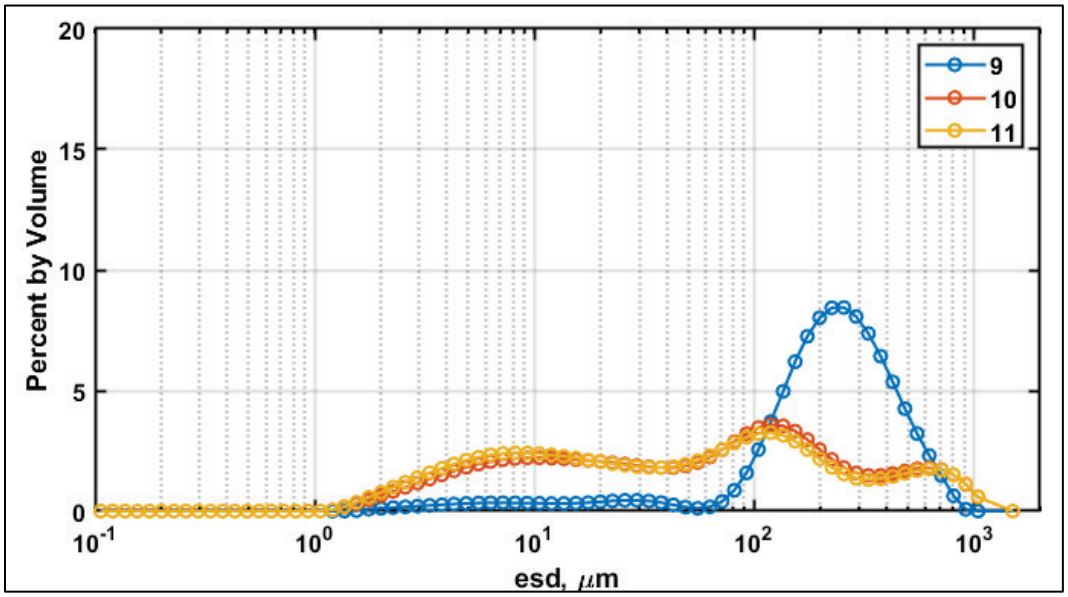

Figure A-4. Grain size distribution using equivalent spherical diameter (esd; μm) for boring samples at Creighton Narrows for DM 156 (13), DM 155A (14), and DM 156 (15).

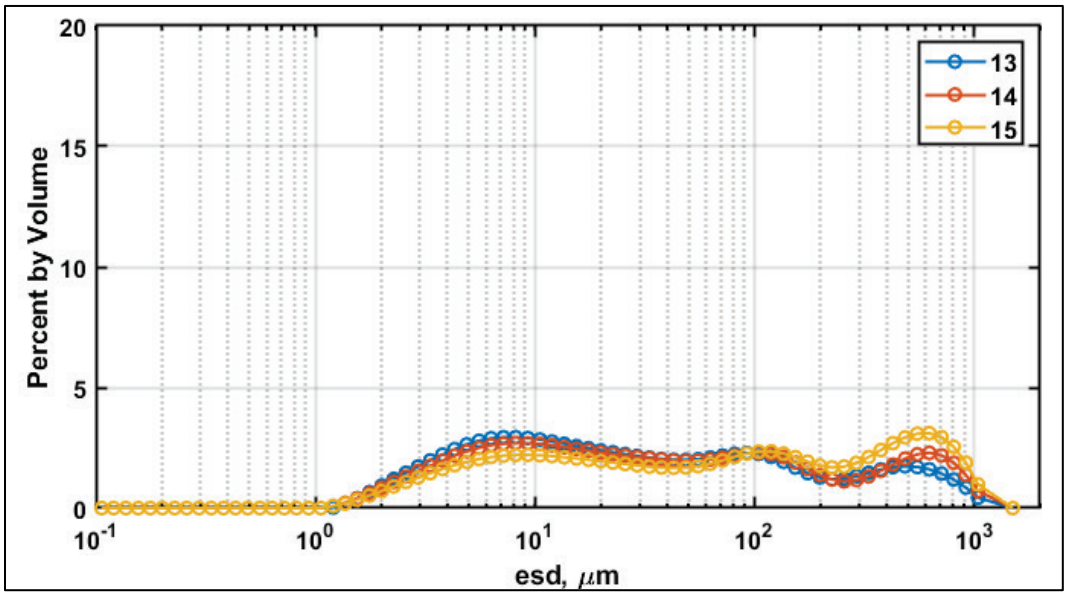

Figure A-5. Grain size distribution using equivalent spherical diameter (esd; μm) for boring samples at Doboy Sound DM 178 (16), and Rockdedundy for DM 184 (17) and DM 188 (18).

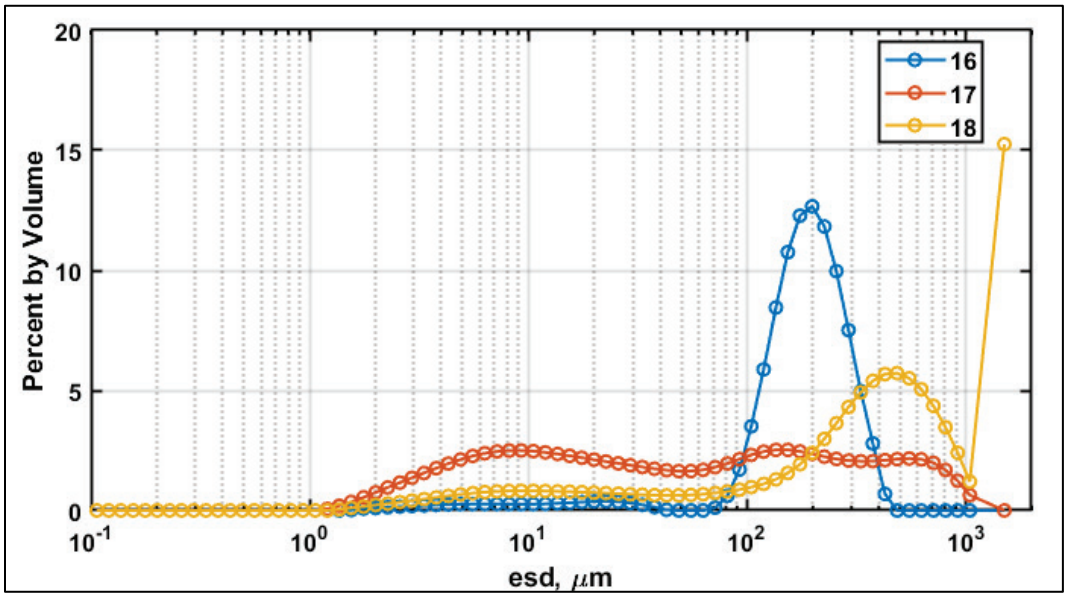

Figure A-6. Grain size distribution using equivalent spherical diameter (esd; μm) for boring samples at Little Mud for DM 190 (19), DM 192 (20), and DM 194 (21).

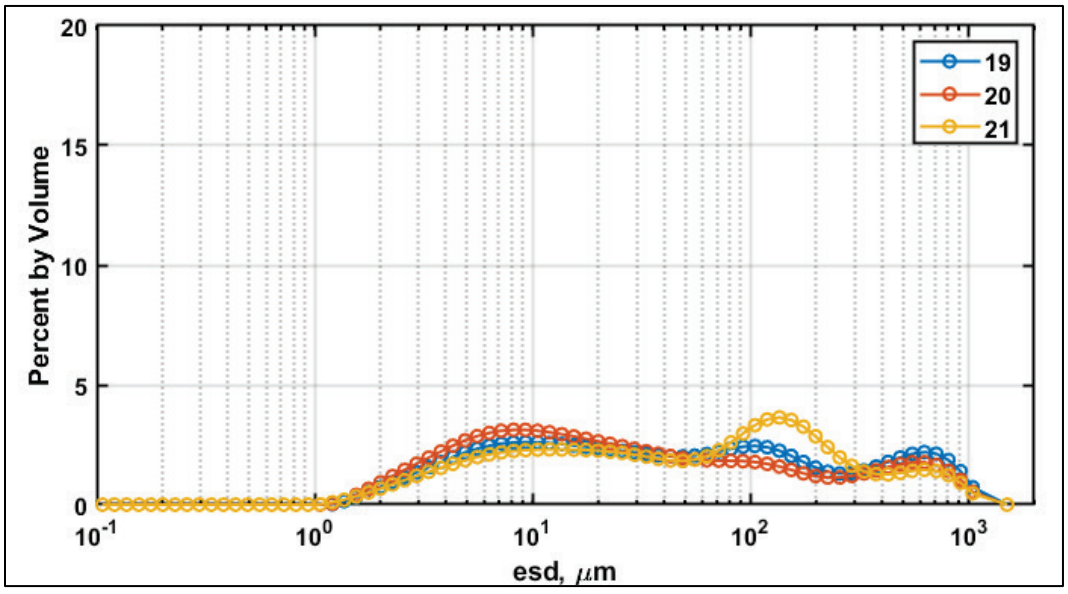

Figure A-7. Grain size distribution using equivalent spherical diameter (esd; μm) for boring samples at Altamaha Sound for DM 204-206 (22) and DM 211 (24), and Buttermilk Sound for DM 220 (26) and DM 222 (27).

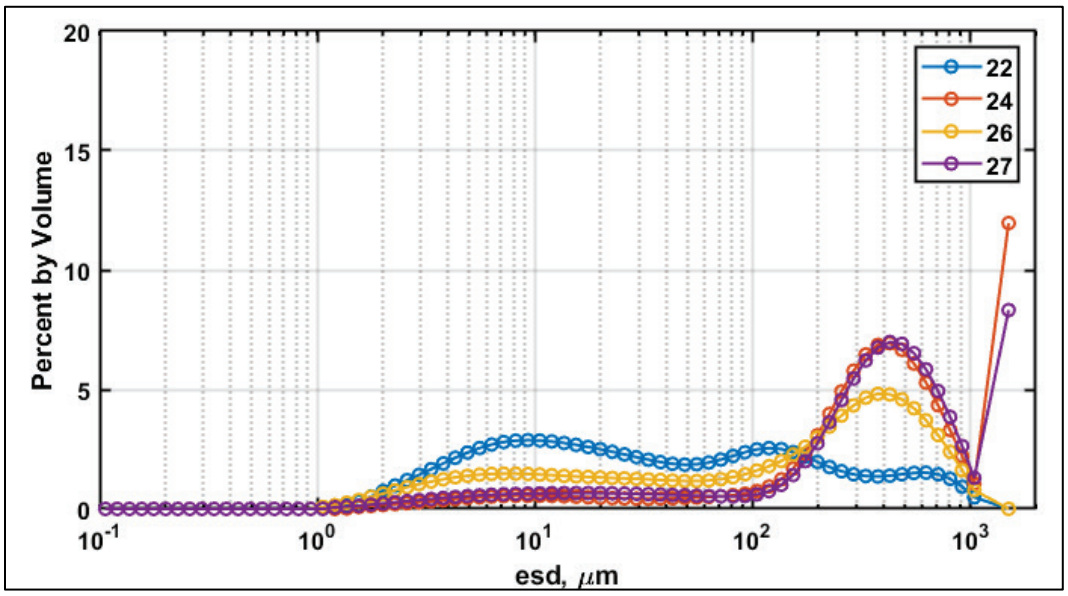

Figure A-8. Grain size distribution using equivalent spherical diameter (esd; μm) for boring samples at McKay River DM 234A (28), Jekyll Creek for the north end (29), DM 13 (30) and DM 19 (31), and Cumberland Sound RG (33).

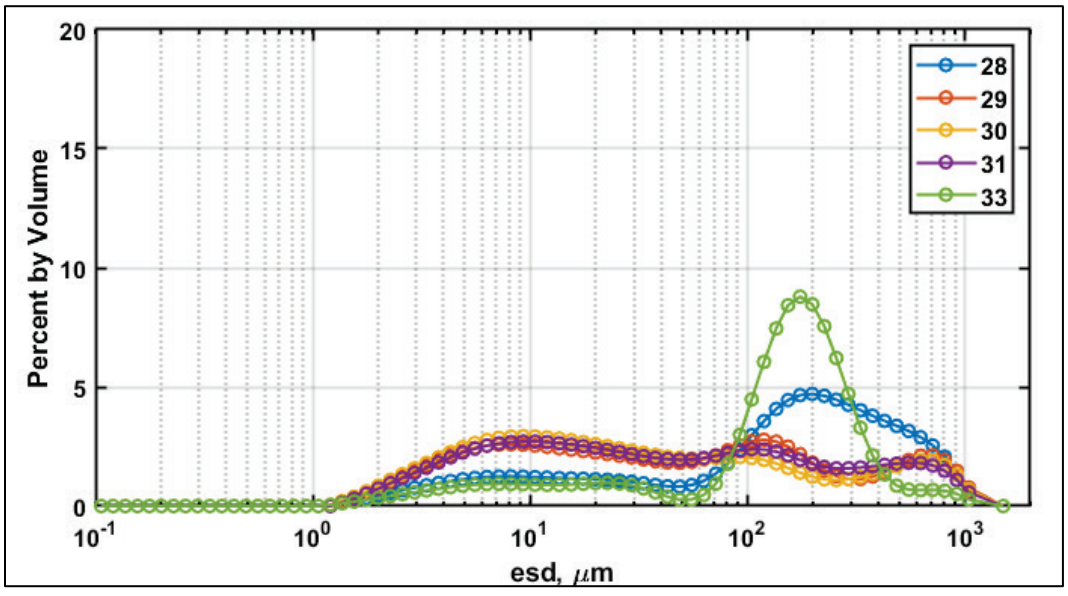

Figure A-9. Grain size distribution using equivalent spherical diameter (esd; μm) for boring samples with >98% sand at Florida Passage DM 102 (12), Altamaha Sound DM 208 (23), Buttermilk Sound DM 218 (25), Cumberland Dividings DM 60 (32), and Cumberland Sound DM 75 (34).

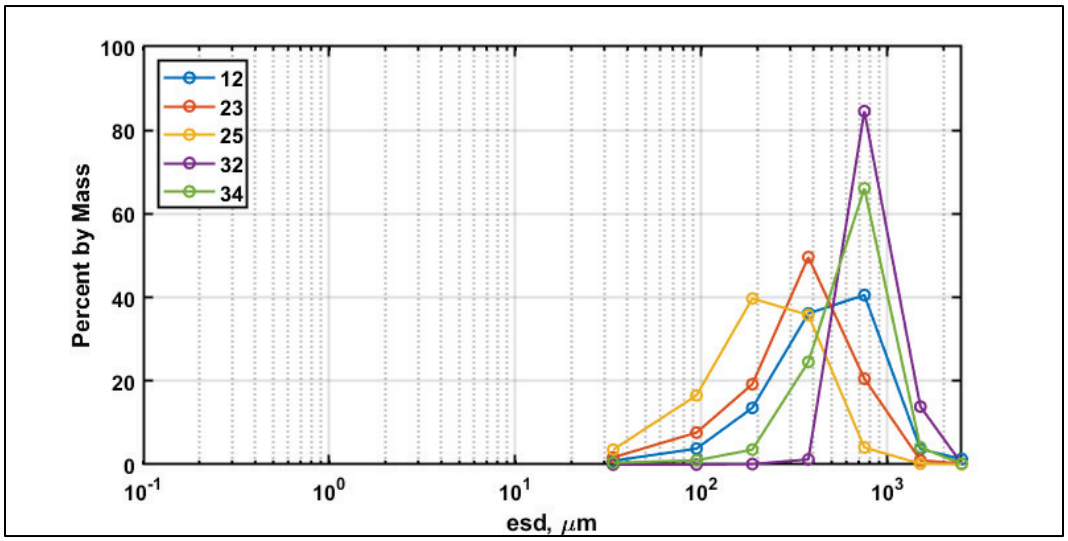

Appendix B: Core Descriptions

Appendix B includes core photographs, descriptions, and depths of physical sample collection during erosion testing (Tables B-1 through B-6).

Table B-1. Core description for Cumberland Sound RG.

Photograph	Description
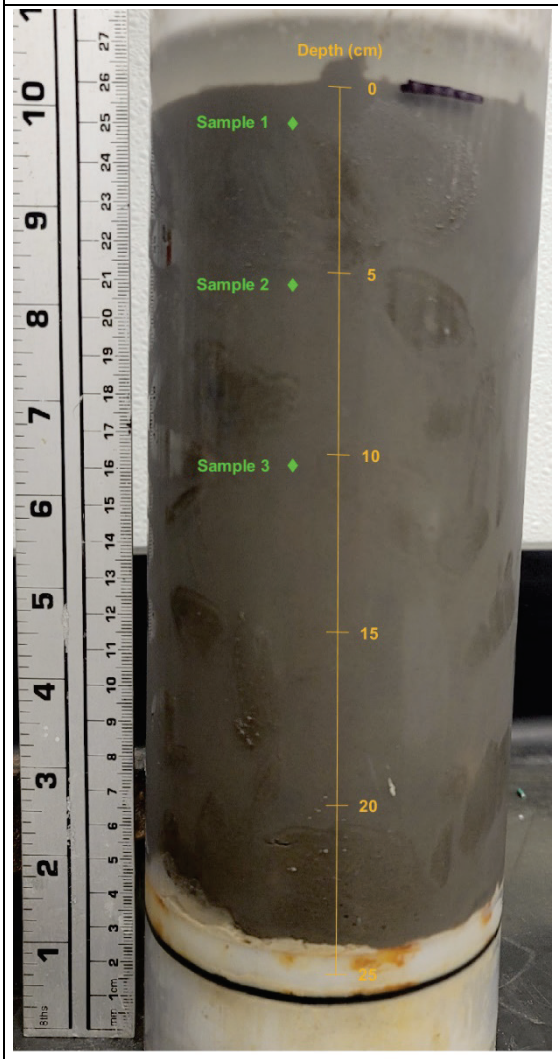	Overlying Water
	Dark brown in color throughout the sediment core. There were no visible voids or cracks on the core. The surface was slightly sloped with a thin oxidized layer <1 mm in thickness.

Table B-2. Core description for Northend Fields Cut.

Photograph	Description
	Overlying Water
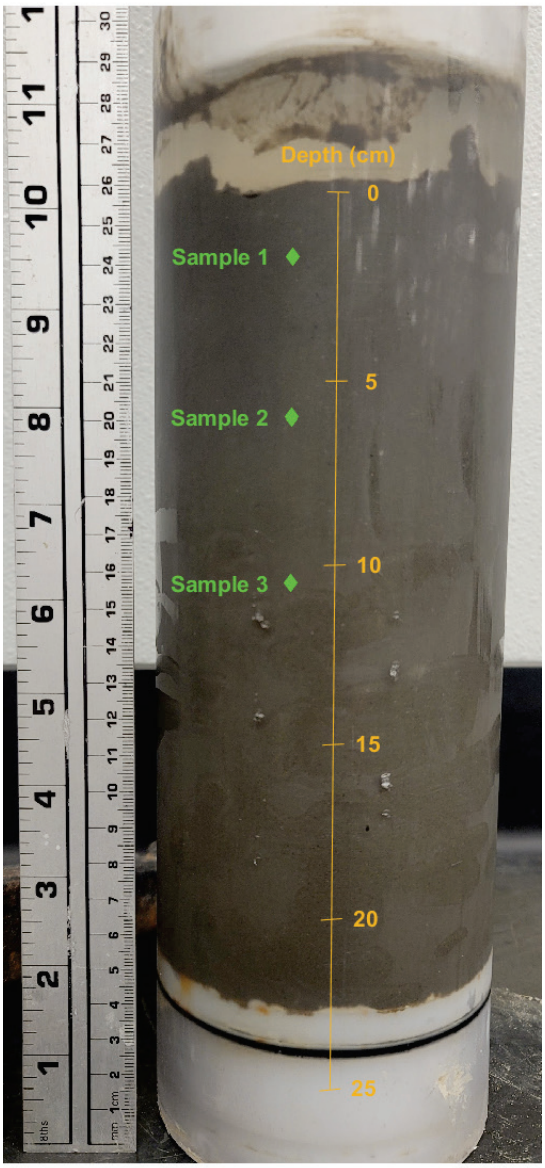	Dark brown in color throughout the sediment core. There were no visible voids or cracks on the core. The surface was uneven with a thin oxidized layer <1 mm in thickness.

Table B-3. Core description for Creighton Narrows DM 156.

Photograph	Description
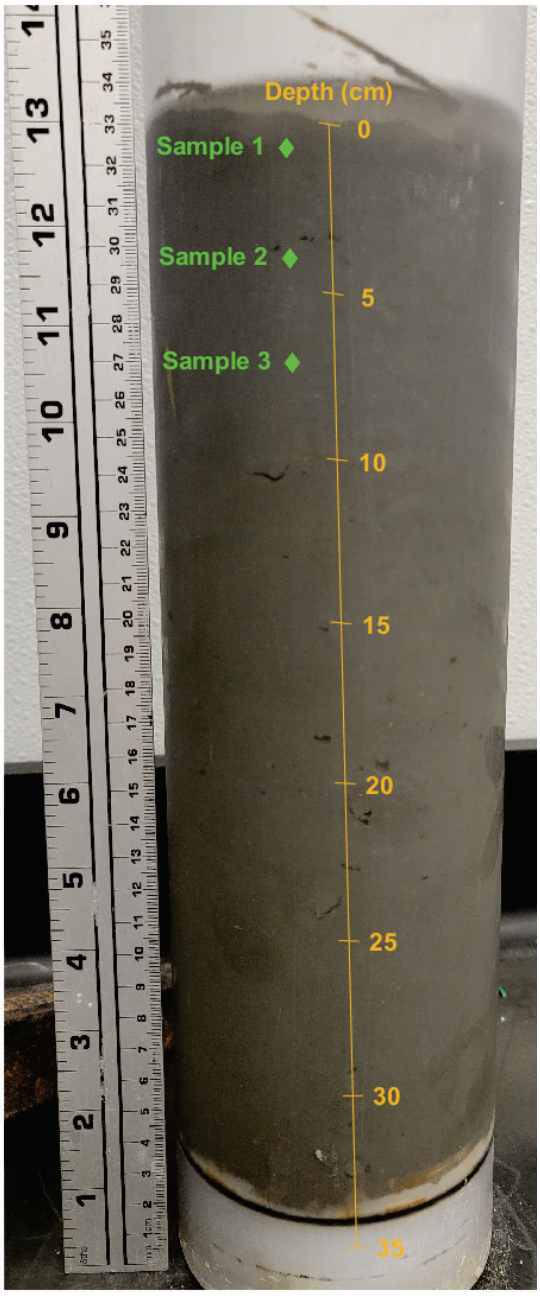	Overlying Water
	Dark brown in color throughout the sediment core. Small voids were visible ~1-10 mm in diameter throughout the core. The surface was slightly sloped with a thin oxidized layer <1 mm in thickness.

Table B-4. Core description for Hell Gate DM 89.

Photograph	Description
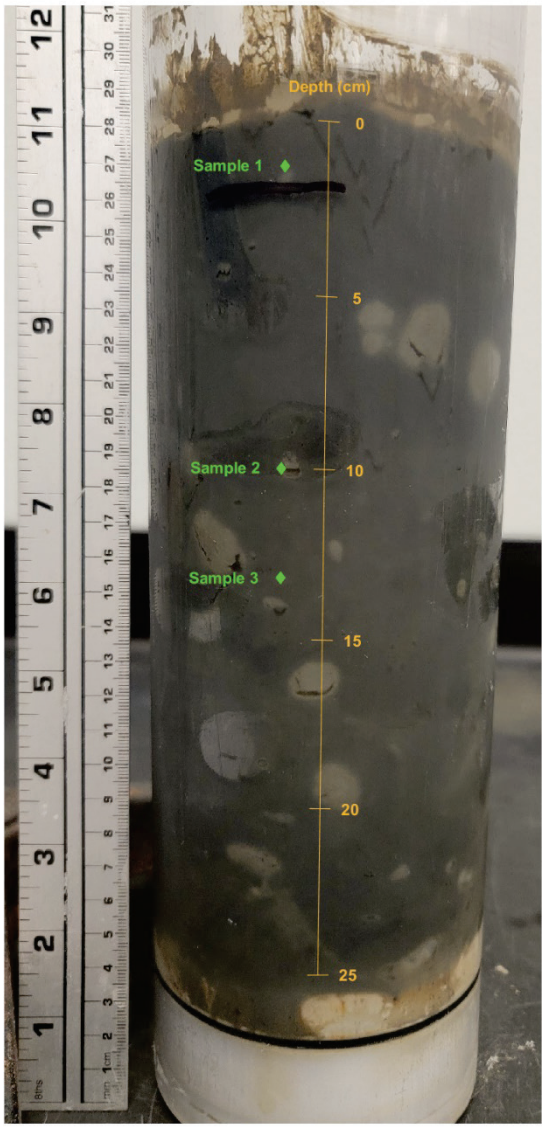	Overlying Water
	Dark grey/black in color throughout the sediment core. Sparsely spaced air voids 1 – 2 cm in diameter were visible throughout the core. The surface was sloped, smooth and had a thin oxidized layer < 1mm in thickness.

Table B-5. Core description for Jekyll Creek DM 19.

Photograph	Description
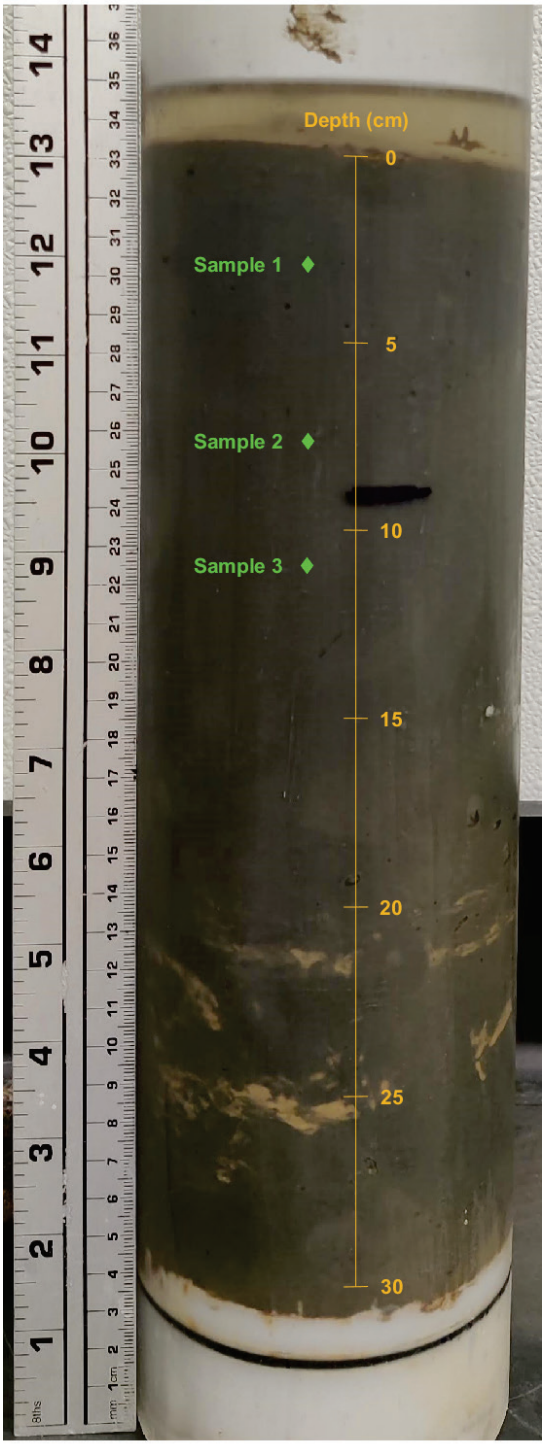	Overlying Water
	Dark grey/black in color throughout the majority of the core. Oxidation coloration at ~20 cm depth, indicating a layer of air bubbles. Sparsely spaced air voids 0.5 – 2 cm in diameter were visible throughout the core. There was a grey oxidized surface layer <1 mm thick.

Table B-6. Core Description for Altamaha Sound DM 204-206

Photograph	Description
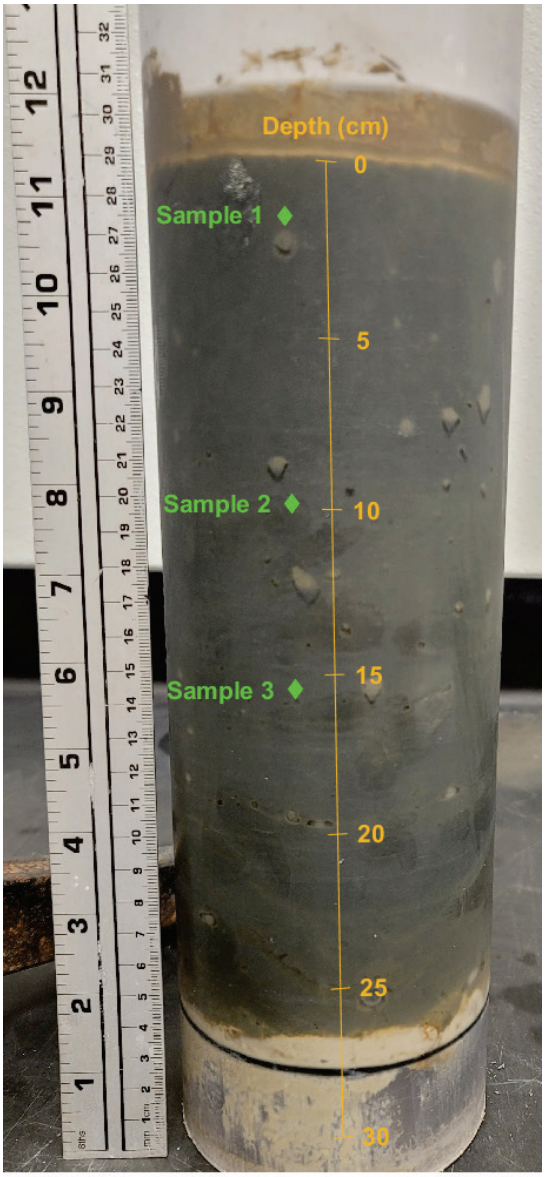	Overlying Water
	Dark grey/black in color throughout core. A crack ~20cm in length was visible just below the surface. Sparsely spaced voids <1cm in diameter were visible throughout the core. The surface was smooth with a thin oxidized layer <1mm thick.

Appendix C: GHD Atlantic Intracoastal Waterway Sediment Sampling & Analysis Report

The 34 core borings analyzed in this study were collected by GHD Inc. as part of an SAS Task order (W912HN21F2011). As part of that contract, GHD Inc. prepared a written report describing the sampling and analysis of those borings. The complete report can be found at http://dx.doi.org/10.21079/11681/44825.

Abbreviations

AIWW	Atlantic Intracoastal Waterway
BUDM	Beneficial Use of Dredged Material
CHL	Coastal and Hydraulics Laboratory
ERDC	US Army Engineer Research and Development Center
esd	Equivalent spherical diameters
FICS	Flume Imaging Camera System
GSD	Grain size distributions
LDPSA	Laser Diffraction Particle Size Analysis
LOI	Loss-On-Ignition
PI	Plasticity Index
SAS	Savannah District
SCC	Suspended sediment concentration
USACE	US Army Corps of Engineers

REPORT DOCUMENTATION PAGE

Form Approved
OMB No. 0704-0188

1. REPORT DATE	2. REPORT TYPE	3. DATES COVERED *(From - To)*
July 2022	Final Report	FY21—FY22

4. TITLE AND SUBTITLE

Using Geophysical and Erosion Properties to Identify Potential Beneficial Use Applications for Atlantic Intracoastal Waterway Sediments

5a. CONTRACT NUMBER

5b. GRANT NUMBER

5c. PROGRAM ELEMENT NUMBER

6. AUTHOR(S)

David W. Perkey, Danielle R. N. Tarpley, and Renée M. Styles

5d. PROJECT NUMBER

5e. TASK NUMBER

5f. WORK UNIT NUMBER

7. PERFORMING ORGANIZATION NAME(S) AND ADDRESS(ES)
Coastal and Hydraulics Laboratory
US Army Engineer Research and Development Center
3909 Halls Ferry Road
Vicksburg, MS 39180-6199

8. PERFORMING ORGANIZATION REPORT NUMBER

ERDC/CHL TR-22-14

9. SPONSORING/MONITORING AGENCY NAME(S) AND ADDRESS(ES)
Regional Sediment Management Program
US Army Engineer Research and Development Center
Vicksburg, MS 39180-6199

10. SPONSOR/MONITOR'S ACRONYM(S)
RSM

11. SPONSOR/MONITOR'S REPORT NUMBER(S)

12. DISTRIBUTION/AVAILABILITY STATEMENT
Approved for public release; distribution is unlimited.

13. SUPPLEMENTARY NOTES
Funding Account code U4375439; AMSCO Code 008303

14. ABSTRACT

In an effort to identify alternative and beneficial use placement strategies for dredged sediments from the Atlantic Intracoastal Waterway (AIWW), the US Army Corps of Engineers, Savannah District (SAS), and the US Army Engineer Research and Development Center (ERDC) performed a series of physical property tests of 34 core borings from the SAS AIWW. Physical property testing found that 14 of the borings were non-cohesive sandy materials that may be suitable for potential beach renourishment or berm construction. The remaining 20 borings had mud contents sufficient enough to result in cohesive behavior. A subset of six of these materials from across the geographic region were further evaluated to characterize their erosion behavior.

Following a self-weight consolidation period of 30 days, erosion testing showed that the tested cohesive sediments had critical shear stress values that ranged from 1.7 Pa to 2.9 Pa, suggesting that these sediments would likely be resistant to erosion in most wetland environments after placement. Additionally, the cohesive sediments were found to produce gravel-sized mud clasts. These clasts could account for 20% or more of the eroded mass and significantly reduce the amount of silts and clays incorporated in suspended plumes during and immediately following placement.

15. SUBJECT TERMS
Atlantic Intracoastal Waterway, Dredging, Dredging spoil—Management, Dredging spoil—Testing, Marine sediments--Testing

16. SECURITY CLASSIFICATION OF:			17. LIMITATION OF ABSTRACT	18. NUMBER OF PAGES	19a. NAME OF RESPONSIBLE PERSON
a. REPORT	b. ABSTRACT	c. THIS PAGE			David W. Perkey
Unclassified	Unclassified	Unclassified	SAR	68	19b. TELEPHONE NUMBER *(Include area code)* 601-634-2736